IOWA STATE UNIVERSITY
Digital Repository

Graduate Theses and Dissertations

Iowa State University Capstones, Theses and Dissertations

2020

Effectiveness of geogrids in roadway construction by large scale laboratory tests

Guangfan Zheng
Iowa State University

Follow this and additional works at: https://lib.dr.iastate.edu/etd

Recommended Citation

Zheng, Guangfan, "Effectiveness of geogrids in roadway construction by large scale laboratory tests" (2020). *Graduate Theses and Dissertations*. 18259.
https://lib.dr.iastate.edu/etd/18259

This Thesis is brought to you for free and open access by the Iowa State University Capstones, Theses and Dissertations at Iowa State University Digital Repository. It has been accepted for inclusion in Graduate Theses and Dissertations by an authorized administrator of Iowa State University Digital Repository. For more information, please contact digirep@iastate.edu.

www.manaraa.com

Effectiveness of geogrids in roadway construction by large scale laboratory tests

by

Guangfan Zheng

A thesis submitted to the graduate faculty

in partial fulfillment of the requirements for the degree of

MASTER OF SCIENCE

Major: Civil Engineering (Geotechnical Engineering)

Program of Study Committee:
Vernon Schaefer, Co-major Professor
Junxing Zheng, Co-major Professor
In-Ho Cho

The student author, whose presentation of the scholarship herein was approved by the program of study committee, is solely responsible for the content of this thesis. The Graduate College will ensure this thesis is globally accessible and will not permit alterations after a degree is conferred.

Iowa State University

Ames, Iowa

2020

Copyright © Guangfan Zheng, 2020. All rights reserved.

www.manaraa.com

TABLE OF CONTENTS

Page

LIST OF FIGURES iv

LIST OF TABLES viii

ACKNOWLEDGMENTS ix

ABSTRACT x

CHAPTER 1. INTRODUCTION 1
- Background 1
- Geosynthetics Introduction 2
- Geogrid Introduction 5

CHAPTER 2. LITERATURE REVIEW 7

CHAPTER 3. TEST SECTION PREPARATION 11
- Integrated Mobile Accelerated System 11
- Loading pattern 13
- Selection of the Instrumentations 16
- Geogrid Preparation 17
- Subgrade Preparation 20
- Base Layer Preparation 21
- Surface Layer Preparation 22

CHAPTER 4. MATERIAL PROPERTIES 23
- Asphalt surface 23
- Base Course Layer 23
- Subgrade 24

CHAPTER 5. TEST RESULTS AND PLOTS 25
- Loading Pattern vs. EPC data 26
  - GE0 Control Section 26
  - GE 1 27
  - GE 2 28
  - GE 4 30
  - GE 5 31
  - GE 7 32
  - GE 12 34
  - GE 15 35
- Loading Pattern vs. Strain 36
  - GE 1 36
  - GE 2 38
  - GE 4 40
  - GE 5 42

www.manaraa.com

GE 7 44
GE 12 46
GE 15 48
Permanent Deformation 50

CHAPTER 6. TEST RESULT ANALYSIS 52

CHAPTER 7. CONCLUSION 55

REFERENCES 57

APPENDIX A. PROPERTIES OF BASE SOILS 59

APPENDIX B. PROPERTIES OF SUBGRADE SOILS 60

www.manaraa.com

LIST OF FIGURES

Page

Figure 1-1 Comparison Between Pavement With and Without the Geosynthetic (Brigham 2019) 3

Figure 1-2 Main Functions of the Geosynthetic in Pavement (Zornberg 2017) 4

Figure 1-3 Three Types of Geogrid: (a) Uniaxial Geogrid; (b) Biaxial Geogrid; (c) Triaxial Geogrid 6

Figure 3-1 Integrated Mobile Accelerated Test System for Laboratory Test (Ingios Geotechnical Inc) 12

Figure 3-2 The Test Configuration in IMAS Device 12

Figure 3-3 Details for Test Sections 15

Figure 3-4 The Selected Instrumentations: (a)Laser LVDT; (b)Earth Pressure Cell; (c)Strain Gauges in Different Size; (d)Strain Data Logger 16

Figure 3-5 Layout for the Location of the Strain Gauge for Biaxial Geogrid 18

Figure 3-6 Strain Gauge Sensors Installation Procedures: (a) Cutting the geogrid into the proper size;(b) Stabilizing the geogrid onto the form; (c) Setting the location of the strain gauge; 18

Figure 3-7 Procedures on Subgrade Preparation: (a) Adding soil layer by layer; (b) Compaction after each layer; (c) Tapping with a temper; (d) Cleaning the surface; (f) Leveling the surface 20

Figure 3-8 Procedures on Base Layer Preparation: (a) Placing the geogrid; (b) Adding the Class 5 aggregate; (c) Leveling the surface; (d) Compacting the base layer with a compactor 21

Figure 3-9 Procedures on Surface Preparation: (a)Placing form layer; (b) Placing the loading plate; (c) Installing the steel plates; (d) Connect all the sensors to the acquisition system 22

Figure 4-1 Steel Plates 23

Figure 5-1 GE0 Control Section- Loading vs. EPC: (a)Test details; (b) Overall EPC data vs. Time; (c) Loading pattern vs. EPC in time interval 0-500 second;(d) Loading pattern vs. EPC in time interval 2000-2500 second; (e) Loading

www.manaraa.com

pattern vs. EPC in time interval 30000-30500 second; (f) Loading pattern vs. EPC in time interval 45000-45500 second; (g) Loading pattern vs. EPC in time interval 60000-60500 second 26

Figure 5-2 GE1- Loading vs. EPC: (a)Test details; (b) Overall EPC data vs. Time; (c) Loading pattern vs. EPC in time interval 0-500 second;(d) Loading pattern vs. EPC in time interval 2000-2500 second; (e) Loading pattern vs. EPC in time interval 30000-30500 second; (f) Loading pattern vs. EPC in time interval 45000-45500 second; (g) Loading pattern vs. EPC in time interval 60000-60500 second 27

Figure 5-3 GE2- Loading vs. EPC: (a)Test details; (b) Overall EPC data vs. Time; (c) Loading pattern vs. EPC in time interval 0-500 second;(d) Loading pattern vs. EPC in time interval 2000-2500 second; (e) Loading pattern vs. EPC in time interval 30000-30500 second; (f) Loading pattern vs. EPC in time interval 45000-45500 second; (g) Loading pattern vs. EPC in time interval 60000-60500 second 28

Figure 5-4 GE4- Loading vs. EPC: (a)Test details; (b) Overall EPC data vs. Time; (c) Loading pattern vs. EPC in time interval 0-500 second;(d) Loading pattern vs. EPC in time interval 2000-2500 second; (e) Loading pattern vs. EPC in time interval 30000-30500 second; (f) Loading pattern vs. EPC in time interval 45000-45500 second; (g) Loading pattern vs. EPC in time interval 60000-60500 second 30

Figure 5-5 GE5- Loading vs. EPC: (a)Test details; (b) Overall EPC data vs. Time; (c) Loading pattern vs. EPC in time interval 0-500 second;(d) Loading pattern vs. EPC in time interval 1100-1600 second; (e) Loading pattern vs. EPC in time interval 27000-27500 second; (f) Loading pattern vs. EPC in time interval 40000-40500 second; (g) Loading pattern vs. EPC in time interval 60000-60500 second 31

Figure 5-6 GE7- Loading vs. EPC: (a)Test details; (b) Overall EPC data vs. Time; (c) Loading pattern vs. EPC in time interval 0-500 second;(d) Loading pattern vs. EPC in time interval 2000-2500 second; (e) Loading pattern vs. EPC in time interval 30000-30500 second; (f) Loading pattern vs. EPC in time interval 45000-45500 second; (g) Loading pattern vs. EPC in time interval 60000-60500 second 32

Figure 5-7 GE12- Loading vs. EPC: (a)Test details; (b) Overall EPC data vs. Time; (c) Loading pattern vs. EPC in time interval 0-500 second;(d) Loading pattern vs. EPC in time interval 2000-2500 second; (e) Loading pattern vs. EPC in time interval 30000-30500 second; (f) Loading pattern vs. EPC in time interval

www.manaraa.com

45000-45500 second; (g) Loading pattern vs. EPC in time interval 60000-60500 second 34

Figure 5-8 GE15- Loading vs. EPC: (a)Test details; (b) Overall EPC data vs. Time; (c) Loading pattern vs. EPC in time interval 0-500 second;(d) Loading pattern vs. EPC in time interval 2000-2500 second; (e) Loading pattern vs. EPC in time interval 30000-30500 second; (f) Loading pattern vs. EPC in time interval 45000-45500 second; (g) Loading pattern vs. EPC in time interval 60000-60500 second 35

Figure 5-9 GE1 Loading Pattern vs. Strain for both direction: (a) Overall Strain vs. Time;(b) Time interval from 0-500 second; (c) Time interval from 2000-2500 second; (d) Time interval from 30000-30500 second; (e) Time interval from 45000-45500 second; (f) Time interval from 60000-60500 second..... 36

Figure 5-10 GE2 Loading Pattern vs. Strain for both direction: (a) Overall Strain vs. Time;(b) Time interval from 0-500 second; (c) Time interval from 2000-2500 second; (d) Time interval from 30000-30500 second; (e) Time interval from 45000-45500 second; (f) Time interval from 60000-60500 second..... 38

Figure 5-11 GE4 Loading Pattern vs. Strain for both direction: (a) Overall Strain vs. Time;(b) Time interval from 0-500 second; (c) Time interval from 2000-2500 second; (d) Time interval from 30000-30500 second; (e) Time interval from 45000-45500 second; (f) Time interval from 60000-60500 second..... 40

Figure 5-12 GE5 Loading Pattern vs. Strain for both direction: (a) Overall Strain vs. Time;(b) Time interval from 0-500 second; (c) Time interval from 2000-2500 second; (d) Time interval from 30000-30500 second; (e) Time interval from 45000-45500 second; (f) Time interval from 60000-60500 second..... 42

Figure 5-13 GE7 Loading Pattern vs. Strain for both direction: (a) Overall Strain vs. Time;(b) Time interval from 0-500 second; (c) Time interval from 2000-2500 second; (d) Time interval from 30000-30500 second; (e) Time interval from 45000-45500 second; (f) Time interval from 60000-60500 second..... 44

Figure 5-14 GE12 Loading Pattern vs. Strain for both direction: (a) Overall Strain vs. Time;(b) Time interval from 0-500 second; (c) Time interval from 2000-2500 second; (d) Time interval from 30000-30500 second; (e) Time interval from 45000-45500 second; (f) Time interval from 60000-60500 second..... 46

Figure 5-15 GE15 Loading Pattern vs. Strain for both direction: (a) Overall Strain vs. Time;(b) Time interval from 0-500 second; (c) Time interval from 2000-2500 second; (d) Time interval from 30000-30500 second; (e) Time interval from 45000-45500 second; (f) Time interval from 60000-60500 second..... 48

www.manaraa.com

Figure 5-16 Permanent Deformation vs. Number of Cycles for Each Test Section 51

Figure 6-1 Relationship Between Direction and Strength in Biaxial Geogrid 53

www.manaraa.com

LIST OF TABLES

Page

Table 1 Loading Level in the Test (Ingios Geotechnical Inc)..... 14

www.manaraa.com

ACKNOWLEDGMENTS

I would like to express my deep gratitude to my academic advisors, Dr. Vernon Schaefer, and Dr. Junxing Zheng, for their patience, support, and encouragement throughout the course of this research. Their professional advice and scientific guidance greatly contributed to my study and the success in this research. I would like to say thanks to Dr. In-Ho Cho for serving on my dissertation committee. I am grateful for your time and valuable comments.

I am very appreciative of Dr. David White, president for Ingios Geotechnical Inc, for his scholastic advice, technical assistance, and offering the test equipment during the experimental program.

I wish to thank Mr. Hossein Alimohammadi as well for being my research teammate during this memorable journey. Without your unconditional help and support, this dissertation would not have been accomplished.

Special thanks to Tensar Corporation for donating the geogrids in this research program.

www.manaraa.com

ABSTRACT

Geogrids have been widely used in the roadway construction as reinforcement in pavement foundations. Geogrids have been effective in practice for reducing rutting damage, distributing traffic loads within the pavement foundation layers, increasing the resilient modulus of base course, improving drainage, reducing differential freeze/thaw problems, and stabilization effects on the subgrade layer. How to accurately evaluate structural benefits of geogrids in pavement foundation is a difficult issue because many factors can affect structural benefits, such as geogrid stiffness, geogrid aperture and rib shape, aperture and rib sizes, the geogrid location/depth, hot mix asphalt thicknesses, base aggregate quality, stiffness thicknesses, and subgrade stiffness.

In this research, we used an Integrated Mobile Accelerated Test System (IMAS) to evaluate reinforcement effects of geogrids. The IMAS system mainly consists of a 5 ft wide and 3 ft deep rigid box and automatic loading frame. A total of eight test configurations were constructed by varying geogrid types (i.e., light-duty biaxial, heavy-duty biaxial, light-duty triaxial, and heavy-duty triaxial geogrids), geogrid locations in pavement (i.e., at the interface between base and subgrade or in the base course), and base aggregate thicknesses. The IMAS can perform cyclic load tests of pavement foundation sections to a large number of load cycles, which simulates vehicle-loading conditions expected during the service life of a pavement system to evaluate the long-term performance of the pavement structure. Testing results include resilient modulus, and permanent deformation of the pavement foundation for evaluating structural benefits of geogrids as a function of geogrid types, geogrid locations, and base aggregate thicknesses. The results of this research will help better design geogrids in roadways to improve pavement quality, extend pavement service life, and reduce life-cycle costs.

www.manaraa.com

CHAPTER 1. INTRODUCTION

Background

In United States, 64% of the roads are paved, and 95% of them are flexible pavement. A conventional flexible pavement is constructed using bituminous materials and granular materials on top of the subgrade layer. Generally, there are four types of failures would happen within the flexible pavement: the surface deformation, the cracking, the disintegration and surface defects (Arkawazi, 2017), where surface rutting or the permanent deformation and the fatigue cracking are the two principal structural failures. The weak subgrade and base course layer are usually the cause of the surface rutting when the accumulated load is applied. Fatigue cracking is another main failure caused by the repeated stress. A number of reasons can cause failure of the pavement, such as drainage problems, weak subgrade, and low stiffness of the base layer, which the load cannot be uniformly distributed to the subgrade layer. All these pavement distresses decrease the pavement performance and reduce the service life of pavement. Design and construction of the pavement over a weak and moist subgrade layer, which cannot provide sufficient strength, is always a huge problem for pavement/geotechnical engineer. One of the cost-effective methods to solve the problem and improve the behavior of the flexible pavement is using geogrid reinforcement. In addition, geogrid is an environmentally friendly product that has been studied and used extensively over the last two decades as reinforcement. Geogrids provide not only reinforcement to the pavement structures, but also offer advantages which include reducing rutting damage, increasing resilient modulus, and improving drainage of the pavement. With the application of using geogrids, the thickness of base course layer can be reduced, and the service life of the pavement can be extended.

www.manaraa.com

However, although geogrids can provide benefits for flexible pavement, presently there does not exist an accurate analysis on the factors that affect the effectiveness of the geogrid. These factors may be the geogrid stiffness, geogrid aperture and rib shape, aperture and rib sizes, the geogrid location/depth, hot mix asphalt thicknesses, base aggregate quality, stiffness thicknesses, and subgrade stiffness. In this study, the Integrated Mobile Accelerated Test System (IMAS) and the measured physical parameters are used to help determine and evaluate the reinforcement performance of the geogrids.

Geosynthetics Introduction

Geosynthetics are a popular and widely used product in civil engineering, especially in pavement construction. Geosynthetics are classified by the material and the application, and includes geotextiles, geogrids, geocells, geonets, geomembranes, and geocomposites. Geosynthetic products related to geotechnical materials have a lot of advantages: long-term durability, environmentally friendly, and easy installation. Geosynthetic products have been used in roadway system since the beginning of the 1970s.

Generally, there are five main functions of the geosynthetics: Separation, filtration, drainage, containment, and reinforcement. Details for these main functions will be discussed below. There also have other functions such as stiffening, and limitation of crack development (Sharbaf, 2016).

1. The first function of geosynthetics is separation. When placing geosynthetics between the two dissimilar materials, for example, the interface between the base course layer and the subgrade layer, the permeable geosynthetic can maintain and keep the integrity and the functionality of both of the materials intact, (Abu-Farsakah et al. 2009). With the help of the geosynthetics, the mixing between the different layers can be prevented, and each layer can keep their complete structure. This allows pavement distress to be reduced. Figure 1-1 below shows

www.manaraa.com

the function of separation by comparing the pavements with and without the geosynthetics, where the distressed pavement has the mixed material from each layer and the intact pavement has separated asphalt layer, base course layer, and the subgrade.

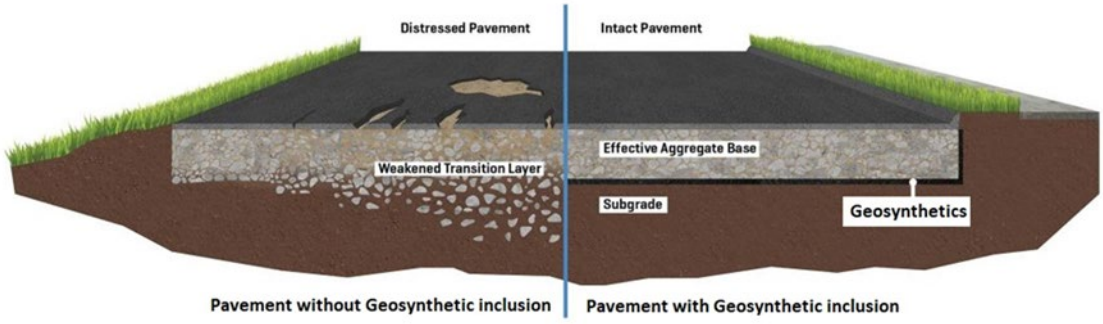

Figure 1-1 Comparison Between Pavement With and Without the Geosynthetic (Brigham 2019)

2. The second function is filtration. The geosynthetics can allow only the liquid flow to pass its plane, and can prevent movement of the soil particles to the other layers. Therefore, the fine particles can remain in its own layer, and the pavement structure can be saved during the service life.

3. The third function is drainage. This function is provided by the geosynthetics transmissivity, which allows gas and liquid to pass and go through within the plane of its structure. The can help to prevent the water remaining inside the pavement system.

4. The fourth function is containment, where the geosynthetics can act like an impervious barrier for both liquid and gas. This hydraulic and gas barrier can limit and minimize the flow and movement in horizontal direction.

5. The last main function of the geosynthetics is reinforcement. The geosynthetics provide the ability to stabilize the soil-geosynthetics composite through developed tensile forces. The geosynthetics inclusion can increase the service life for the pavement especially over weak

www.manaraa.com

subgrade by transferring the overload to the geosynthetics materials. With the help of geosynthetics, two factors of pavement can be improved: the TBR (Traffic Benefit Ratio) and the BCR (Base Course Reduction) ratio. Under the same properties, TBR is the ratio between the reinforced pavement and the unreinforced pavement of the cycle of loads to reach a particular rutting depth. BCR is ratio on the reduction in base course layer thickness between the reinforced and unreinforced pavement when reaching the same pavement distress status under the same material properties. The reinforcement ability in geosynthetics is one of the most important functions, as it extends the service of the pavement, as well as decreases the cost of construction by reducing the base course thickness. These functions are illustrated in Figure 1-2.

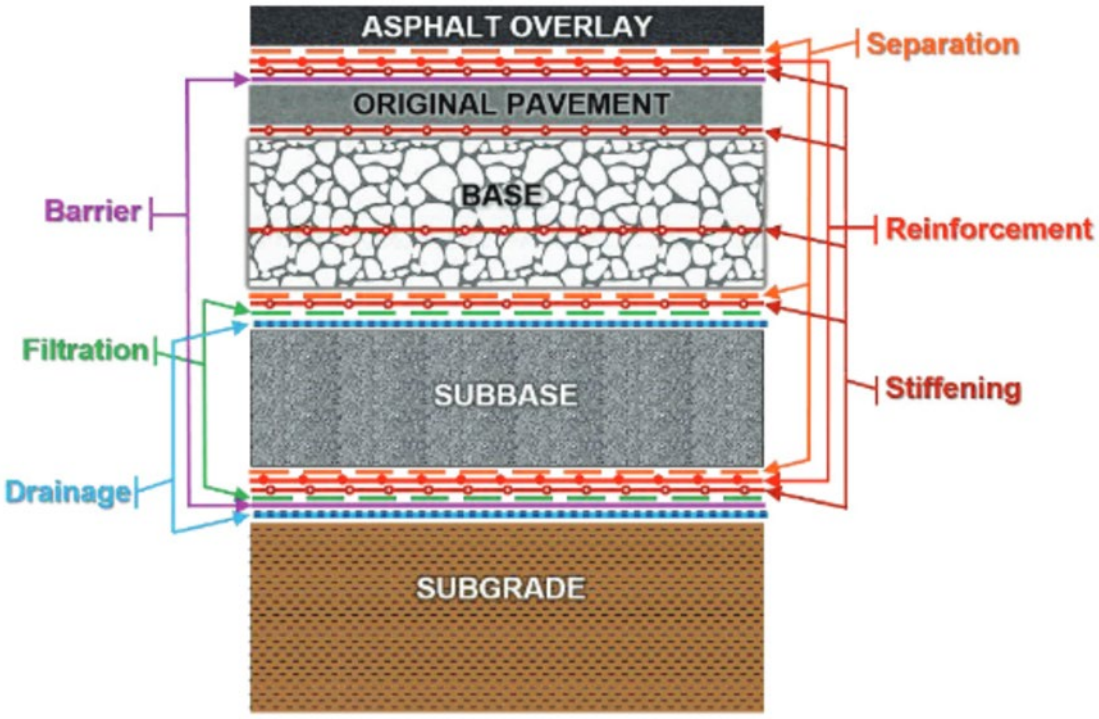

Figure 1-2 Main Functions of the Geosynthetic in Pavement (Zornberg 2017)

www.manaraa.com

Geogrid Introduction

Made of Polypropylene or Polyethylene, geogrids are one of most widely used geosynthetics, used primarily as reinforcement in geotechnical construction. The majority of geogrid products are in 2-dimensional format, which can provide reinforcement in one surface. These 2-dimensional geogrids come in Uniaxial, Biaxial, and Triaxial forms, and are the three well-known types used in geotechnical construction. Uniaxial geogrid has a linear shape which can provided strength in one direction and is usually used for reinforcement in slope and embankment.

Biaxial and Triaxial geogrids are mainly used for reinforcement in pavement construction. They provide strength in two directions and three directions, respectively. The different shaped aperture causes the differences in their properties. Biaxial geogrids have a rectangular aperture. It is popular worldwide because of its high resistance to short-term and moderate dynamic loads, as well its long-time life. The strength is not the same in the two directions because the length is unequal for the geogrid ribs in the two directions.

For triaxial geogrid, the shape of the aperture is triangular, which is the most stable and widely utilized shape in construction. These grids provide strength in three directions compared to the Biaxial geogrid. Because of its geometry, more in-plane stress can be provided in multiple, equilateral directions, and more efficiency can be gained when transferring the stress from aggregate to the stabilizing geogrid. In addition, as it is more cost-effective than biaxial geogrids, it is becoming more popular for designers. The geometry shape of these three types of geogrids are shown in Figure 1-3.

www.manaraa.com

(a)

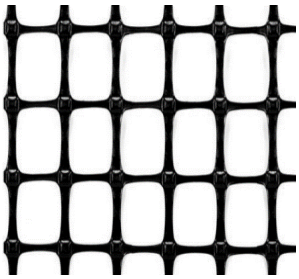

(b)

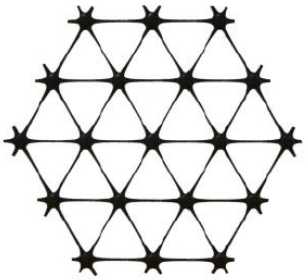

(c)

Figure 1-3 Three Types of Geogrid: (a) Uniaxial Geogrid; (b) Biaxial Geogrid; (c) Triaxial Geogrid

Beside the reinforcement, geogrid products can also provide confinement between the soil particles in base course layer and the geogrid. The opening aperture can offer interlocking forces as the aggregates can lock with the geogrid, therefore, the strength of the support layers to the pavement can be improved. The factors affecting the confinement may be the aperture size and the aggregate particle-size distribution.

In this study, in order to evaluate the effect on the aperture shape and the strength of the geogrid rib, four types of geogrid were used: Light Duty Biaxial – Tensar BX1100, Heavy Duty Biaxial – Tensar BX1200 (Tensar, Tensar Biaxial BX Geogrids,2020), Light Duty Triaxial – Tensar TX130s, and Heavy Duty Triaxial – Tensar TX7 (Tensar, Tensar TriAx Geogrids,2020).

www.manaraa.com

CHAPTER 2. LITERATURE REVIEW

In the last two decades, geogrids have been widely used and countless researches have been conducted in both laboratory and field tests. The strain measurement is an important and necessary task in an engineering test, especially in geogrid measurement when we are doing the mechanics studies. Using strain gauges to measure the strain behavior is a popular way to do the strain measurement. Feng et al. (2014) provided the contrast and analysis on different techniques on the strain measurement by using strain gauges. Three different kinds of measurements for geogrids exist: Dial test indicator, inductive displacement transducer, and replacing the geogrid with other material are compared based on their accuracy. The strain measures were also contrasted according to their process: the preparation work, the sticking technique, the welding technique and the protection technique. His study shows that there are limitations in each of these tests because of the disturbance which occurs before and during the tests, and can affect the results. A recent method called particle image velocimetry can be effective because it is an non-intrusive technique.

Strain gauges are an effective method to measure the development of strain in geosynthetics, and they can provide the accurate result if it's installed in a proper way and correct location. The following researchers studied the effectiveness of geogrids with the help of strain gauges. Hanandeh (2007) performed three sets of testing programs on geosynthetic reinforced materials: rolling wheel load full scaled geosynthetic reinforced test lanes, laboratory cyclic plate loading test and cyclic plate loading on full-scale test lane. Because of the excellent behavior on reliability and cyclic endurance, Vishay strain gauges were selected and installed on the surface of the geogrid to measure the strain during the accelerated loading test. The Vishay strain gauges can quantify the geosynthetics mobilization during the loading process as well. The

www.manaraa.com

installation was on the each side of the rib and waterproofed and protective coating are used in order to reduce the effect on the results. He also used other sensors to collect the loading data and environmental responses. His experimental test results prove that geosynthetics can stabilize the subgrade, reinforce the load built on the weak soil, and reducing the permanent deformation of pavement layers.

In order to investigate the effect of geosynthetic pavement and build a formula equation, Saghebfar (2014) completed eight sections of tests with difference types of woven geotextile which are placed under the granular base layer. Five hundred thousand loading cycle were tested. This study also chose Vishay Micro-Measurements strain gauges on the geotextile, because of its long availability under the loading condition. Silicone adhesion was added to provide waterproof and protect the strain gauges. In addition, three different types of strain gauges were selected to measure the hot mix asphalt behavior: foil strain gages, strain coils and H-bar gauges. They were installed on pavement cores and the top of the asphalt surface. A time domain reflectometers (TDR) sensor was placed on each test to collect the data of temperature and moisture change differs. Finite element models were developed and compared with the experimental tests. His result shows that the geotextile can increase the pavement performance by reducing the rutting and pressure at the top of the subgrade.

Two years later, Sharbaf (2017) performed six similar laboratory tests to evaluate the effectiveness of biaxial and triaxial geogrid-reinforced flexible pavements. A steel cylindrical mold with 6 ft in diameter and 7 ft in height was used in his test, and the geogrids were placed at the mid-depth of aggregate base course and subgrade-base interface separately. Three million repeated loadings were provided by a hydraulic actuator for each test in this study. Foil strain gauges were installed on the ribs of geogrids to measure the flexural and longitudinal strain on

www.manaraa.com

two direction for both type of geogrid. In addition, he also used other instrumentations such as pressure cells and the Linear Variable Differential Transformer (LVDT) to measure the pressure and the displacement respectively. By comparing the results between reinforced and non-reinforced sections, it was found that geogrid can reduce the surface rutting, vertical pressure effectively, and increase the load applications significantly.

Measuring the tension of the geogrid is significant because it is an essential part in reinforcement mechanisms studies. In the study of Chen et al. (2010), strain gauges were attached to the surface of the model geogrid with epoxy resin. The tension was measured during the reinforcement in centrifuge test. Numerical modeling was performed as well to verify the results from the experimental test. The results show that the geogrid plays an important role at resisting the tension during loading, and the Generalized Kelvin model is a effective model to describe the time-dependent and nonlinear behavior of the composite material in a accurate way during the measuring the reinforcement tension.

Geogrids can also help to reinforce the soil structure because of their tensile stiffness. Gnanendran and Selvaduai (2001) used strain gauges to measure the stabilizing force provided by the geogrid in a small-scale laboratory test for sloped fill. Bonded electrical resistance strain gauges were selected in this study, and they were placed in pairs on both the top and the bottom faced of the ribs of geogrid in order to minimize the effect of the flexural strains. Lead wires were covered on the strain gauges as well to reduce the damage during transportation and compaction. The results show that installing the strain gauges in pairs on each face of the geogrid provide a better result than just installing strain gauges in one side. The geometry of the sloped fill and the depth of the geogrid can affect the result of the reinforcement significantly. His study

www.manaraa.com

illustrates a relationship between the tensile force developed in the geogrid and the applied foundation pressure.

Strain gauge cannot only measure the strain behavior on geogrid but also on other engineering projects. Castaneda and Lange (2010) improved and completed test procedures for measuring the residual stresses on in-situ plain concrete pavements. By installing the strain gauges on the concrete slab, stain and temperature data can be measured at initial and ending condition for FAA's NAPTF residual stress testing. Affixed strain gauges provided great help in this study because the slight strain change can be measured under different loading condition. The strain gauge results and three-dimensional Finite Element Model analysis improved the measurement method of the residual stress in plain concrete pavement.

www.manaraa.com

CHAPTER 3. TEST SECTION PREPARATION

Integrated Mobile Accelerated System

The Integrated Mobile Accelerated Test System (IMAS), Figure 3-1, is used to perform the laboratory tests. Cyclic loading with a large number of load cycles, which simulates the vehicle-loading conditions on the pavement foundation, can be performed by the IMAS. In addition, the IMAS can help us determine the resilient modulus, deflection, permanent deformation of the pavement, so that the service life of the pavement system and the long-term performance of the pavement structure can be evaluated as well. The IMAS device has a square base container, where the depth is 3 feet and the length are 5 feet (Figure 3-2). In order to minimize the boundary effects and simulate the stiffness of the natural soils, the rigid wall and foam layer are set up to control the boundary conditions. The load plate system or the hydraulic actuator is above the center of the device to provide the repeated loading during the test. All the sensors are connected to the data acquisition system and the results are recorded during the test for one million cycles.

www.manaraa.com

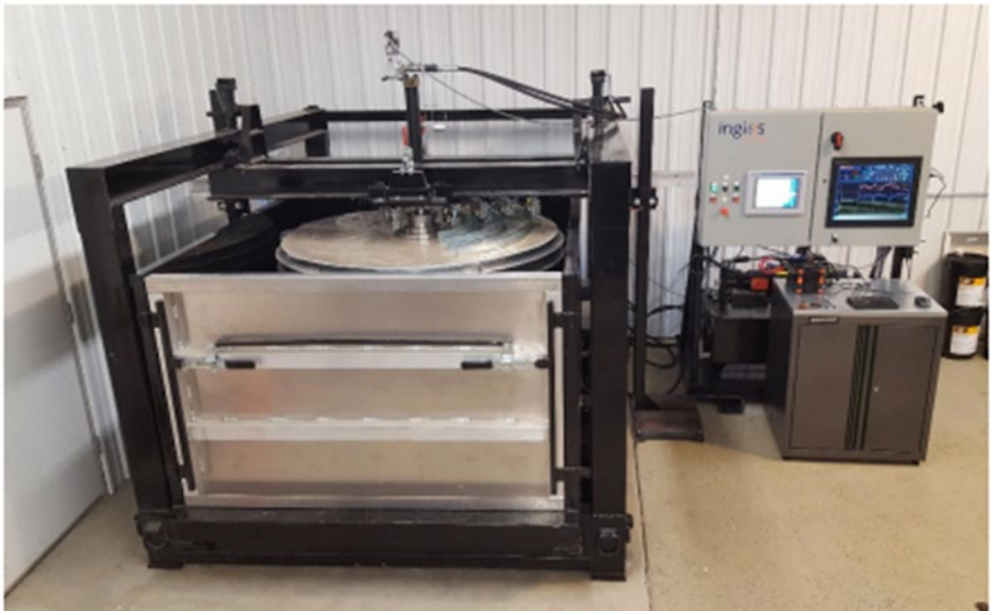

Figure 3-1 Integrated Mobile Accelerated Test System for Laboratory Test (Ingios Geotechnical Inc)

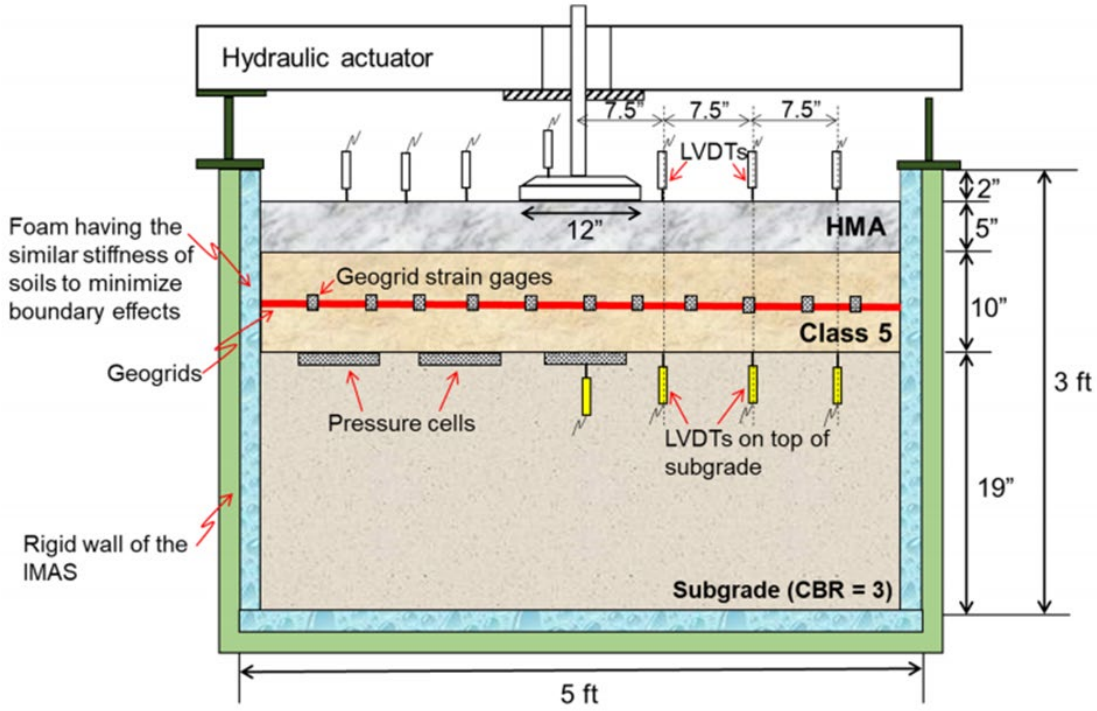

Figure 3-2 The Test Configuration in IMAS Device

www.manaraa.com

Loading pattern

For each test, the load will be provided to the IMAS by a 12-inch diameter loading plate sitting above the center of the container. The hydraulic actuator will enforce the load direct onto the loading plate. For each test section, in order to simulate the real traffic loading, 10 different load vales were stored in the IMAS and are applied randomly during the tests, which meet the ASSTO standard. Although the loading pattern is random, the distribution will follow the same standard distribution for each section, see Table 1. Therefore, the results from each section can be compared. For example, the No.5 loading pattern with a maximum load of 2,539 psi and minimum load of 226 psi will be enforced to each test section 1 and test section 5 with the same distribution of 16%. Totally, 100,000 cycles loading are applied in each section with a cyclic load pulse time of 0.15 second and dwell time of 0.85 second. The total time for each cycle is one second. Each test takes approximately 17 hours. Table 1 provides the detail information of the loading pattern with their magnitude, number of cycles, the distribution, and the forcing and relaxing time.

Introduction for Test Sections

Eight test sections were performed in this test in order to evaluate the pavement behavior using different types of geogrid and under different location: GE0, GE1, GE2, GE4, GE5, GE7, GE12 and GE15. GE0 is the control section so no geogrid was installed in this section. Biaxial geogrid was used in GE1, GE2 and GE5; and Triaxial geogrid were used in GE4, GE7, GE12 and GE15. For GE1, GE2, GE4, and GE12, the geogrid products were placed at the interface between the base course layer and the subgrade layer; for GE5 and GE7, the geogrid was installed at the middle of the base course layer. In addition, both light duty and heavy-duty geogrid products were used in the test as well. The details for the test sections are shown in Figure 3-3 below.

www.manaraa.com

Table 1 Loading Level in the Test (Ingios Geotechnical Inc)

No.	Max Load (Lbs.)	Min Load (Lbs.)	Cyclic Stress (Psi)	N Cycles	% Distribution	
1	513	226	2.5	5	5	5,000
2	1,013	226	7.0	8	8	8,000
3	1,526	226	11.5	15	15	15,000
4	2,039	226	16.0	22	22	22,000
5	2,539	226	20.5	16	16	16,000
6	3,052	226	25.0	12	12	12,000
7	3,565	226	29.5	9	9	9,000
8	4,073	226	34.0	6	6	6,000
9	4,586	226	38.5	5	5	5,000
10	5,086	226	43.0	2	2	2,000

Set	100
Total	100,000
Repeat	1,000
Cycle time (s)	1
Time (min)	1,000
Time (hr.)	17

Pulse (s)	Dwell (s)
0.15	0.85

www.manaraa.com

Figure 3-3 Details for Test Sections

www.manaraa.com

Selection of the Instrumentations

Collection of information can help us to compare and evaluate the behavior of the reinforced pavement system with different types of geogrids and determine the optimal location of placing the geogrid. In order to compare the pavement performance between each test sections, it's necessary to record the permanent deformation, the stress at both subgrade and base layer, as well as the strain behavior on the geogrid rib on different directions. These measurements can help us understand the mechanism for the geogrid and pavement. Three instrumentations were selected according to the literature review, the data type, and the cost. The laser LVDT (Linear Variable Differential Transformer) was used to measure the deformation happen on the pavement; the strain gauge was used to measure the strain behavior on the geogrid rib; and the pressure cell was used to record the pressure. Figure 3-4 shows these instruments.

(a) (b)

Figure 3-4 The Selected Instrumentations: (a)Laser LVDT; (b)Earth Pressure Cell; (c)Strain Gauges in Different Size; (d)Strain Data Logger

www.manaraa.com

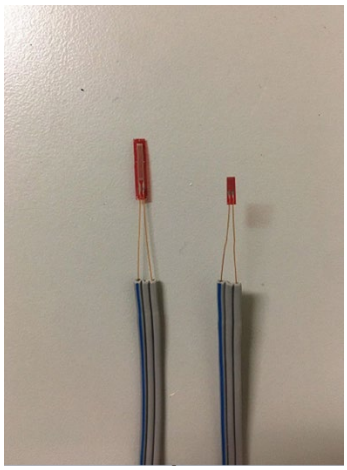

(c)

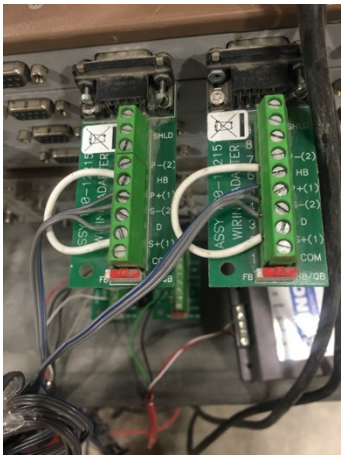

(d)

Figure 3-5.(continued)

Geogrid Preparation

In order to measure the mobilization, and the strain behavior of the geogrid in the pavement section, strain gauges were installed on the top surface of the geogrid in each section. For both triaxial and biaxial, the strain gauges were placed on two direction. For biaxial geogrid, the aperture is in rectangular shape, direction 1 is set at the short side, direction 2 is set at the long side, and the angle between them is 90 degrees. For triaxial geogrid, since the aperture shape is in isosceles triangle, direction 1 and direction 2 were selected randomly because they have the same size and length on the geogrid as well as the junction. Figure 3-5 shows the layout for the strain gauges on the Biaxial geogrid, and Figure 3-6 shows the procedures on installing the strain gauges.

www.manaraa.com

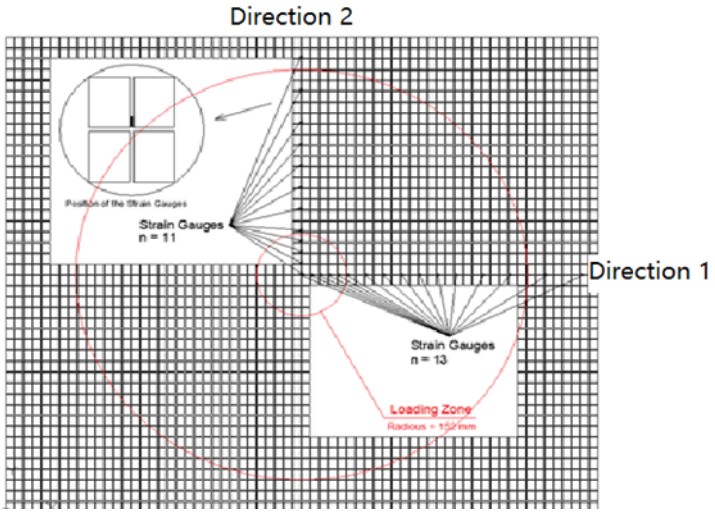

Figure 3-6 Layout for the Location of the Strain Gauge for Biaxial Geogrid

(a) (b)

Figure 3-7 Strain Gauge Sensors Installation Procedures: (a) Cutting the geogrid into the proper size;(b) Stabilizing the geogrid onto the form; (c) Setting the location of the strain gauge; (d) Cleaning the geogrid surface with alcohol and sand paper; (e) Adding primer before installing the strain gauge; (f) Attaching the stain gauge by using glue; (g) Covering with tube for protection

www.manaraa.com

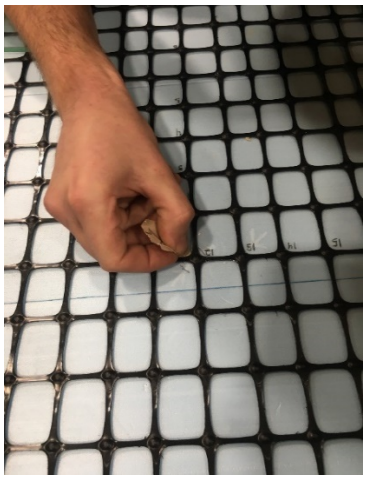

(c)

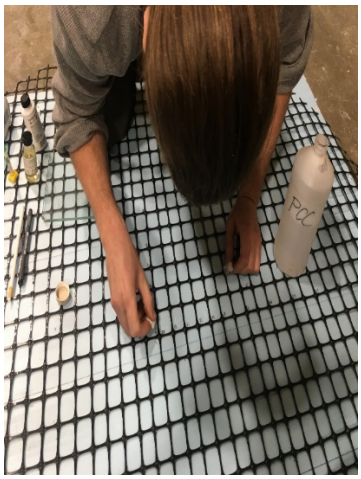

(d)

(e)

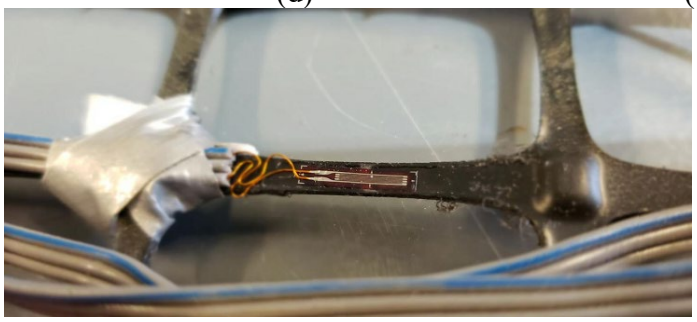

(f)

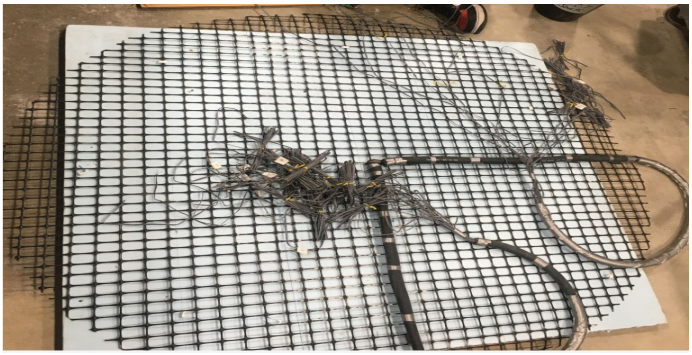

(g)

Figure 3-8. (continued)

www.manaraa.com

Subgrade Preparation

The subgrade soil was added layer by layer in order to reach a uniform condition. A 50-lb hammer was used to provide the compaction after adding each layer. In order to keep the surface flat, a temper was used as well after each compaction. Finally, after cleaning the surface, a spirit level tool was used to measure and leveled the surface. The subgrade preparation process is shown in Figure 3-7.

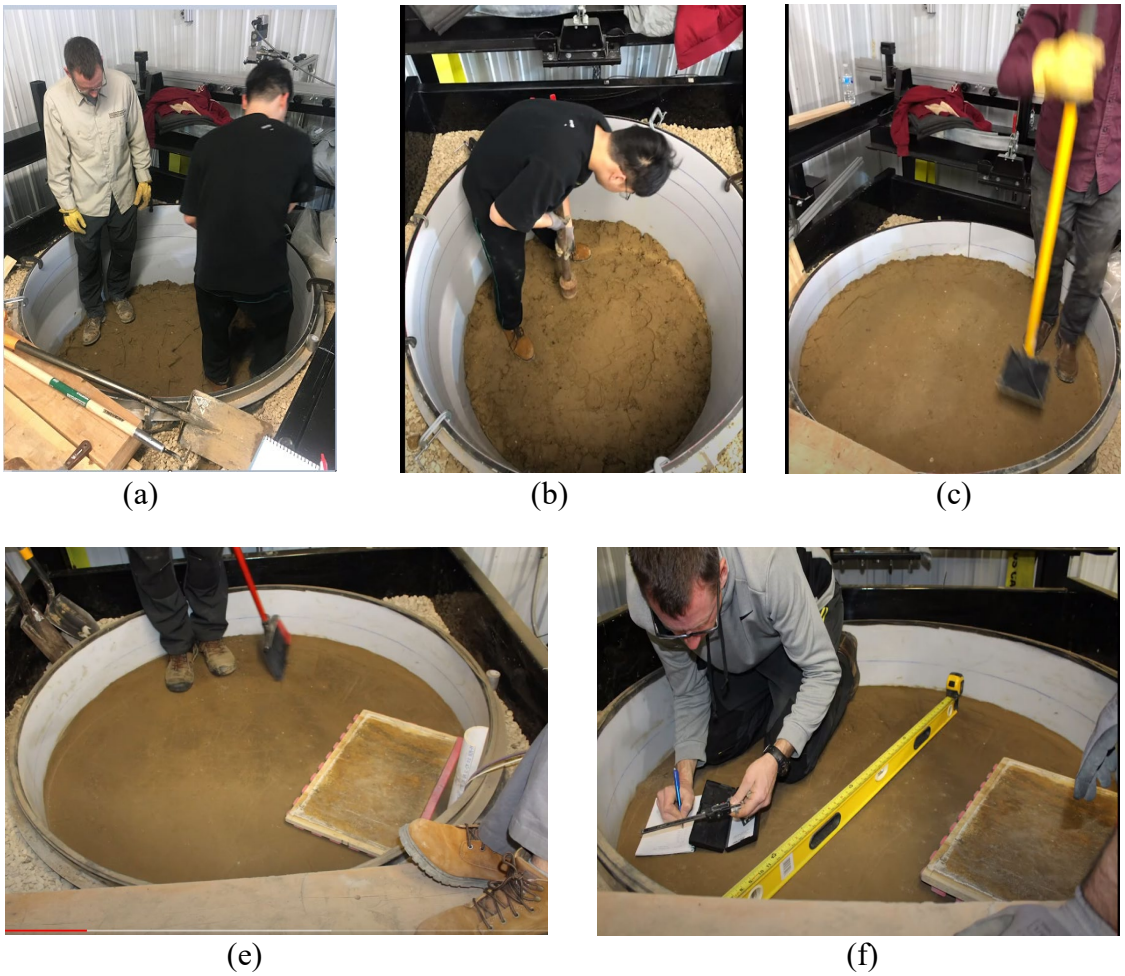

(a) (b) (c)

(e) (f)

Figure 3-9 Procedures on Subgrade Preparation: (a) Adding soil layer by layer; (b) Compaction after each layer; (c) Tapping with a temper; (d) Cleaning the surface; (f) Leveling the surface

www.manaraa.com

Base Layer Preparation

After the subgrade preparation, the geogrid was placed above the subgrade surface. Then the aggregates were poured above the geogrid layer by layer again. Then a rake was used to level the surface as well. After leveling the surface, a compactor was used to provide the compaction on the base layer for three minutes. Figure 3-8 shows the procedures on preparing the base layer.

(a)

(b)

(c)

(d)

Figure 3-10 Procedures on Base Layer Preparation: (a) Placing the geogrid; (b) Adding the Class 5 aggregate; (c) Leveling the surface; (d) Compacting the base layer with a compactor

www.manaraa.com

Surface Layer Preparation

The asphalt surface was replaced by a double layer of steel. And the loading plate was set at the middle of the container. In addition, a thin form layer was placed between the steel and the base layer to provide friction and protection. The final step was to connect all the sensors to the acquisition system. Pictures of the surface layer preparation are shown in Figure 3-9.

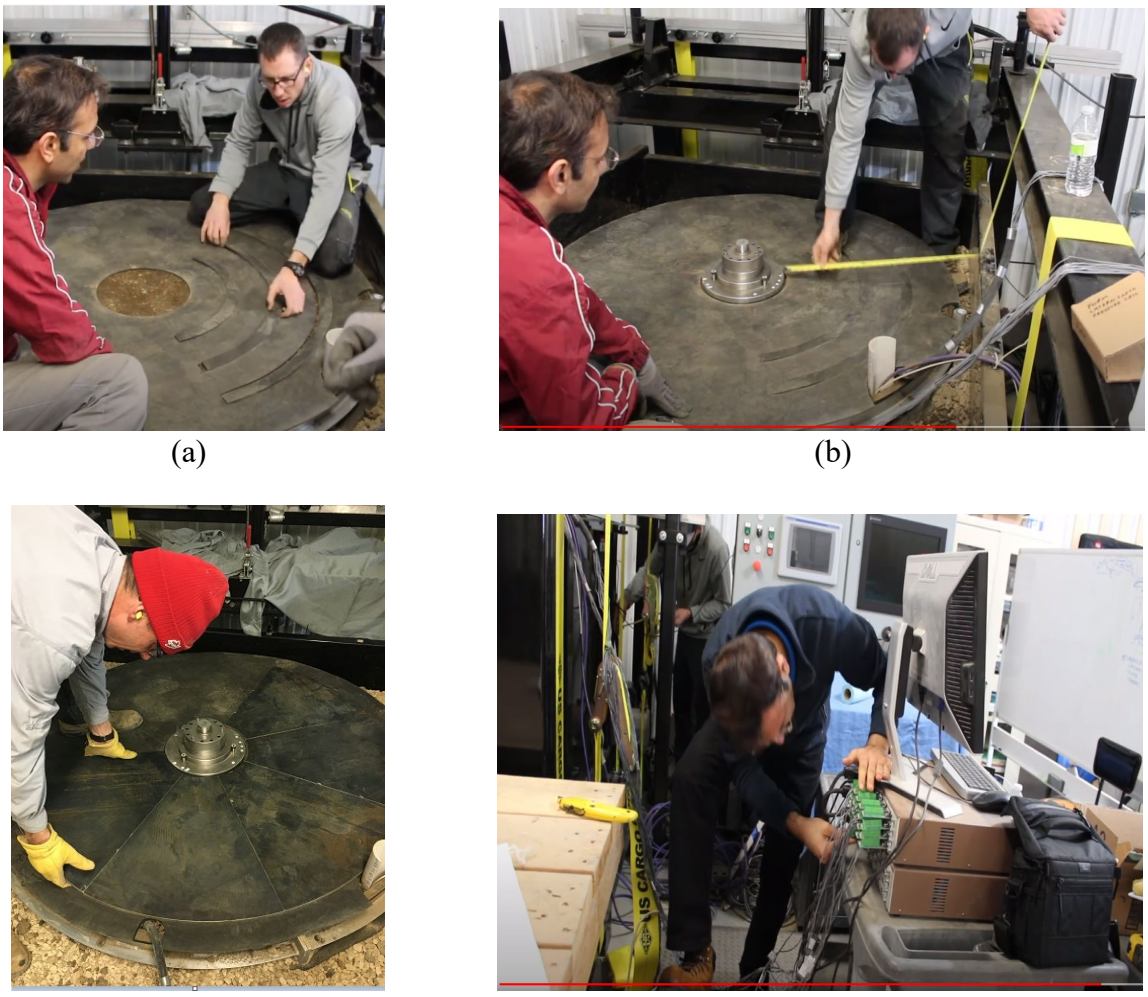

(a) (b)

(c) (d)

Figure 3-11 Procedures on Surface Preparation: (a)Placing form layer; (b) Placing the loading plate; (c) Installing the steel plates; (d) Connect all the sensors to the acquisition system

www.manaraa.com

CHAPTER 4. MATERIAL PROPERTIES

Asphalt surface

During the laboratory tests, it's difficult to pave the asphalt surface on the IMAS system. Therefore, the asphalt layer was substituted by the steel plate (figure 4-1), which can provide the equivalent weight of the real asphalt surface. Double layer of steel was used and each layer has seven pieces of fan-shaped steel.

Figure 4-1 Steel Plates

Base Course Layer

Class 5 aggregates, which are normally used for driveways and the base of construction projects in the state of Minnesota (MnDOT GRADING & BASE MANUAL, 2017), were used for aggregate base layer (see Appendix: Properties of Base Soils). The detailed report for the particle-size distribution curve and the Atterberg limits index values are shown in the Appendix A as well.

www.manaraa.com

Subgrade

The subgrade soil with CBR = 3 will be representative for common subgrade soil condition in Minnesota. To achieve CBR = 3, we prepared the subgrade at a target moisture content of 16.64%. More details for the subgrade soil are presented in Appendix B. The soil was stored in Dr White's lab, which is located in Little Chicago, Minnesota.

www.manaraa.com

CHAPTER 5. TEST RESULTS AND PLOTS

This section collects the pressure data and the strain data from the earth pressure cells and the strain gauges. All the pressure cell data and the strain data are plotted versus the loading pattern for each section. For the pressure cells, the data were collected every 0.005 second; for the strain gauges, the data were recorded every 0.1 second. The loading data were recorded as well for every 0.6 second. All the pressure cell data and strain data are plotted for the whole 100,000 cycles. Besides, in order to look at the details, five time intervals with 500 second duration are selected so that only a small range of data can be focused and analyzed. These five intervals are 0-500 second, where the test started; 2000-2500 second, where the slope of the data plot is changing; 30000-30500 second, where is the middle point of the tests;45000-45500 second, where is the third quarter of the test; and 60000-60500 sec. where is the end of the test. For each test, both the overall data and the specific time interval data are compared and analyzed to evaluate the benefit of geogrid reinforcement.

www.manaraa.com

Loading Pattern vs. EPC data

GE0 Control Section

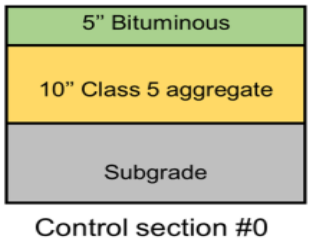

(a)

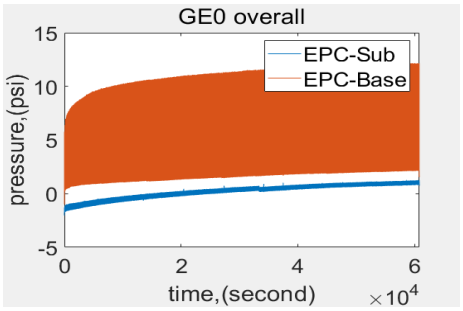

(b)

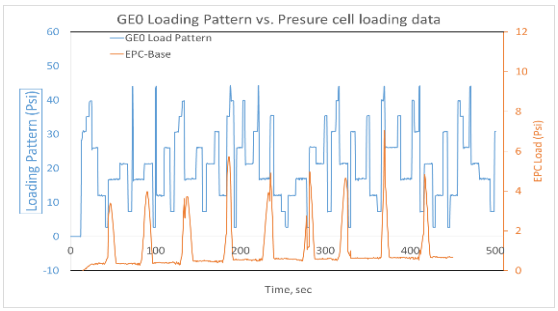

(c)

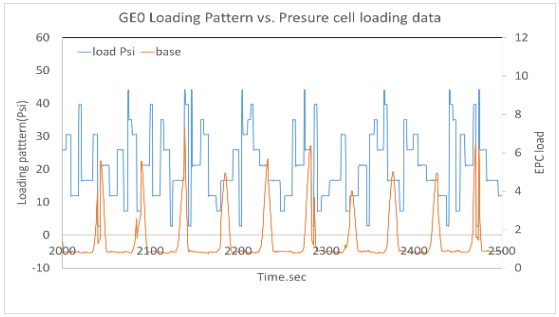

(d)

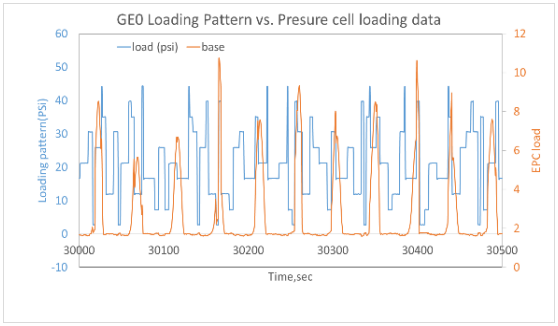

(e)

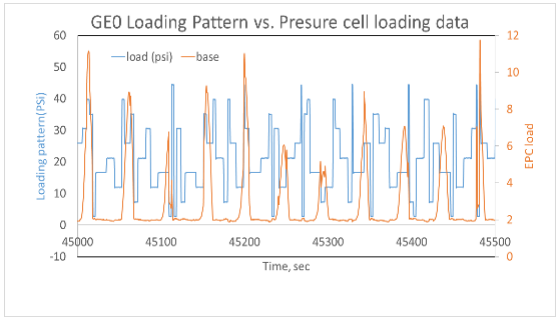

(f)

Figure 5-1 GE0 Control Section- Loading vs. EPC: (a)Test details; (b) Overall EPC data vs. Time; (c) Loading pattern vs. EPC in time interval 0-500 second;(d) Loading pattern vs. EPC in time interval 2000-2500 second; (e) Loading pattern vs. EPC in time interval 30000-30500 second; (f) Loading pattern vs. EPC in time interval 45000-45500 second; (g) Loading pattern vs. EPC in time interval 60000-60500 second

www.manaraa.com

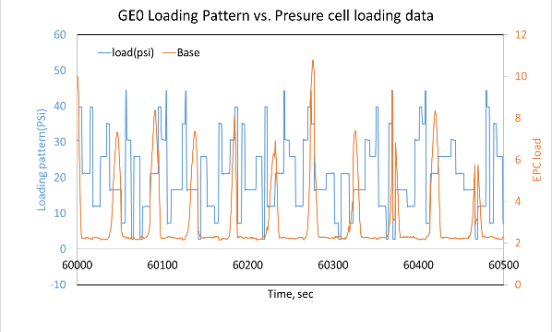

(g)

Figure 5-2. (continued)

GE 1

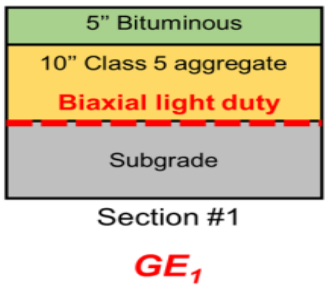

(a)

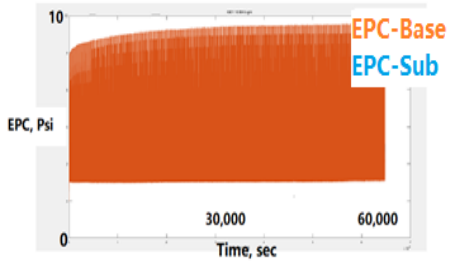

(b)

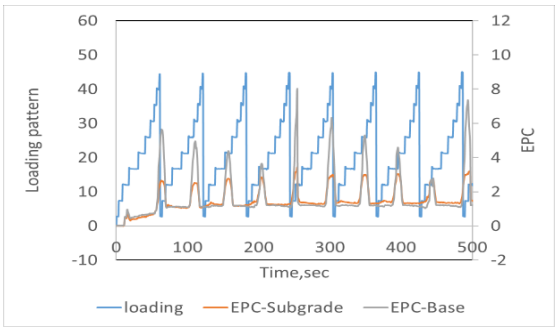

(c)

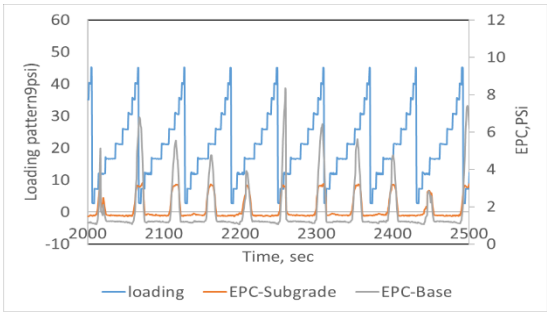

(d)

Figure 5-3 GE1- Loading vs. EPC: (a)Test details; (b) Overall EPC data vs. Time; (c) Loading pattern vs. EPC in time interval 0-500 second;(d) Loading pattern vs. EPC in time interval 2000-2500 second; (e) Loading pattern vs. EPC in time interval 30000-30500 second; (f) Loading pattern vs. EPC in time interval 45000-45500 second; (g) Loading pattern vs. EPC in time interval 60000-60500 second

www.manaraa.com

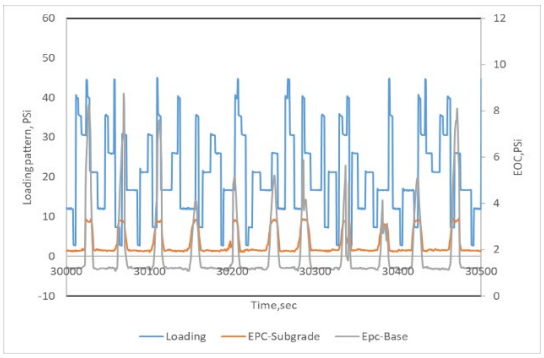

(e)

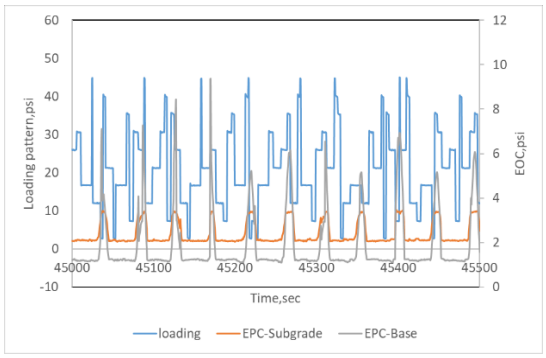

(f)

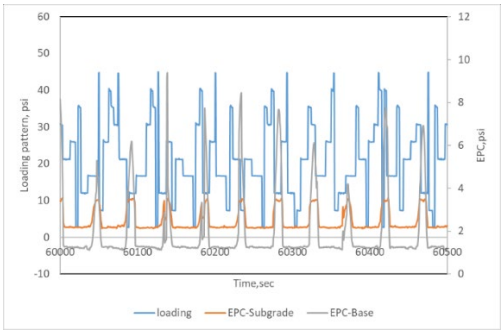

(g)

Figure 5-4. (continued)

GE 2

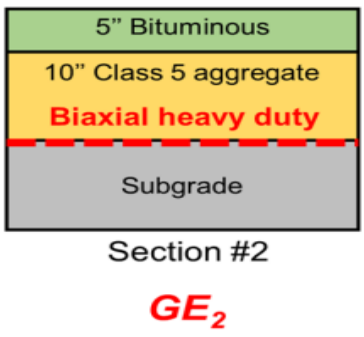

(a)

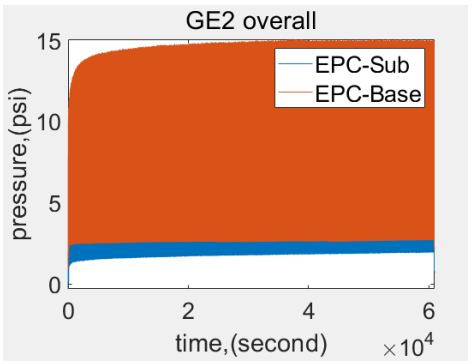

(b)

Figure 5-5 GE2- Loading vs. EPC: (a)Test details; (b) Overall EPC data vs. Time; (c) Loading pattern vs. EPC in time interval 0-500 second;(d) Loading pattern vs. EPC in time interval 2000-2500 second; (e) Loading pattern vs. EPC in time interval 30000-30500 second; (f) Loading pattern vs. EPC in time interval 45000-45500 second; (g) Loading pattern vs. EPC in time interval 60000-60500 second

www.manaraa.com

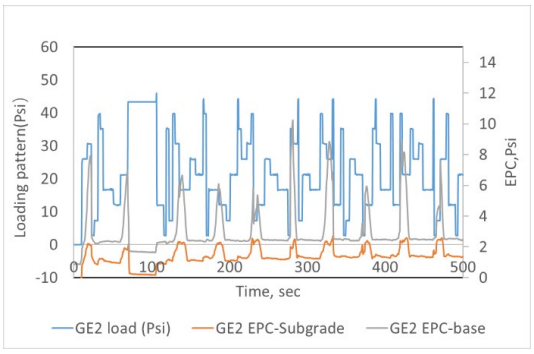

(c)

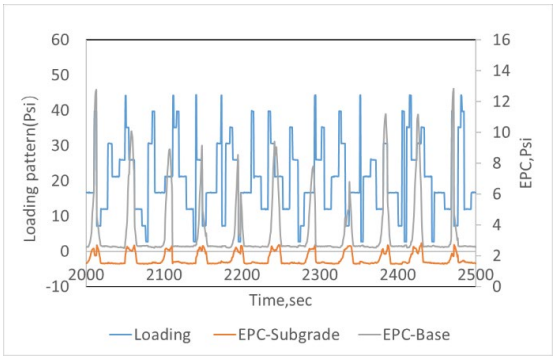

(d)

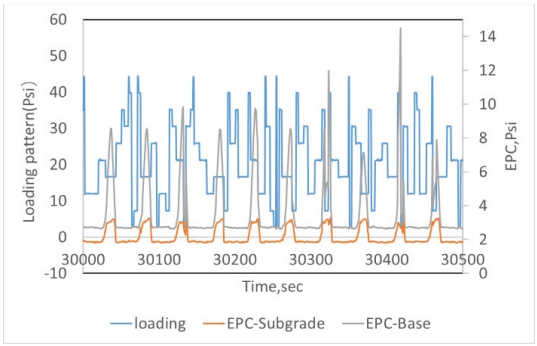

(e)

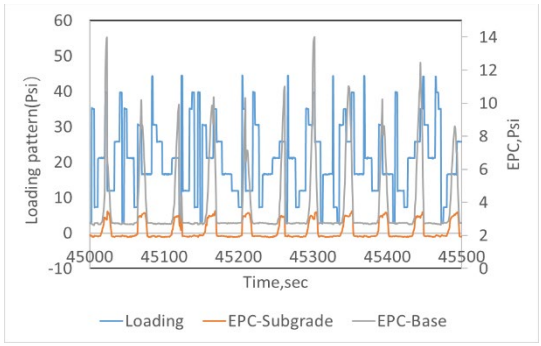

(f)

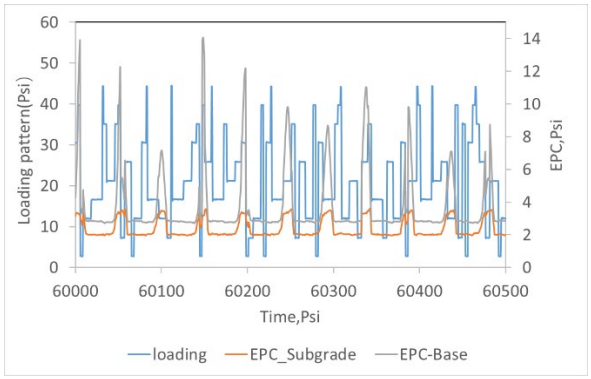

(g)

Figure 5-6. (continued)

www.manaraa.com

GE 4

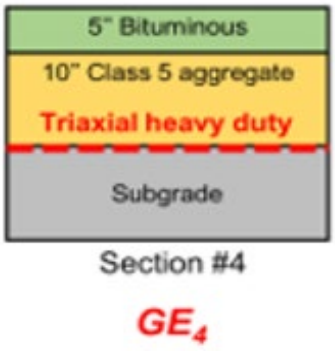

(a)

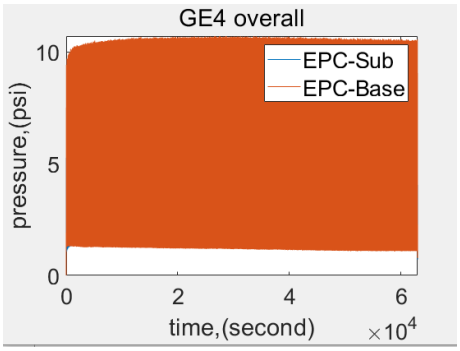

(b)

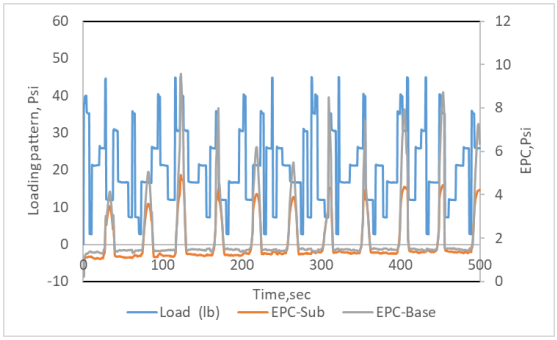

(c)

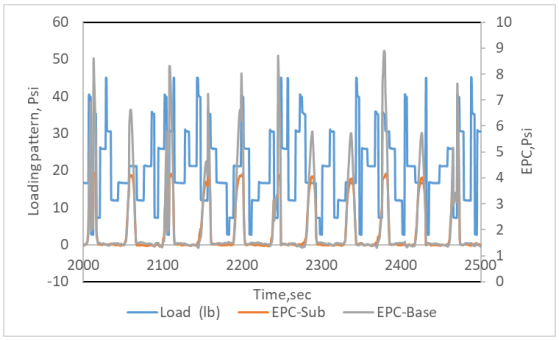

(d)

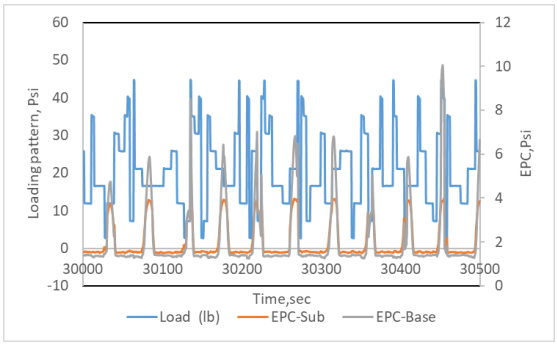

(d)

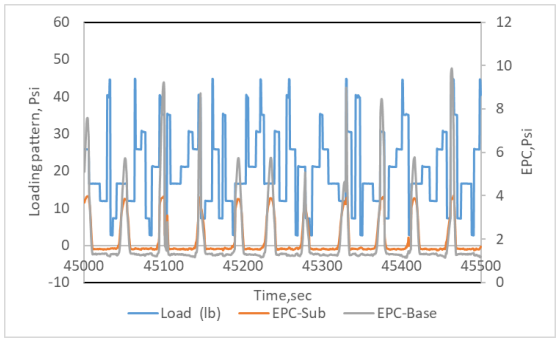

(e)

Figure 5-7 GE4- Loading vs. EPC: (a)Test details; (b) Overall EPC data vs. Time; (c) Loading pattern vs. EPC in time interval 0-500 second;(d) Loading pattern vs. EPC in time interval 2000-2500 second; (e) Loading pattern vs. EPC in time interval 30000-30500 second; (f) Loading pattern vs. EPC in time interval 45000-45500 second; (g) Loading pattern vs. EPC in time interval 60000-60500 second

www.manaraa.com

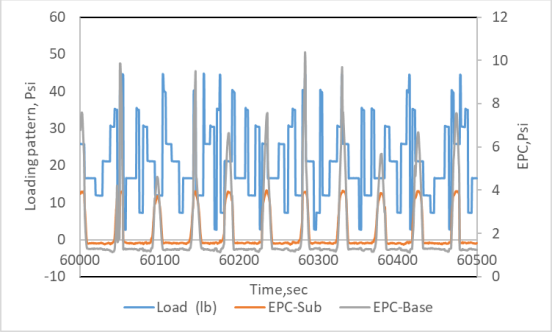

(g)

Figure 5-8.(continued)

GE 5

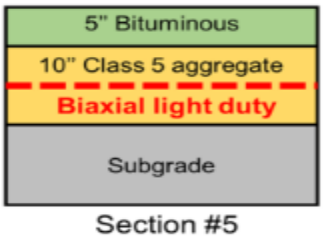

(a)

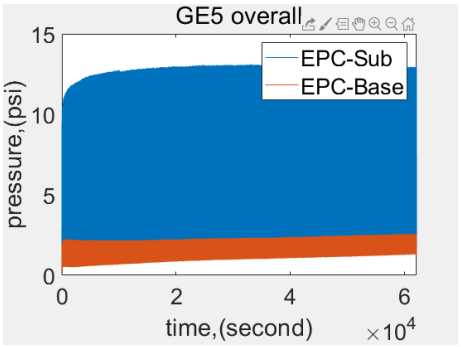

(b)

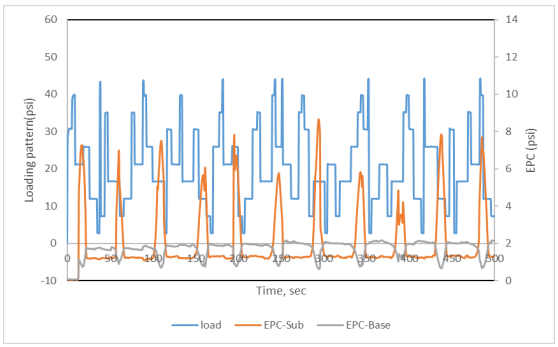

(c)

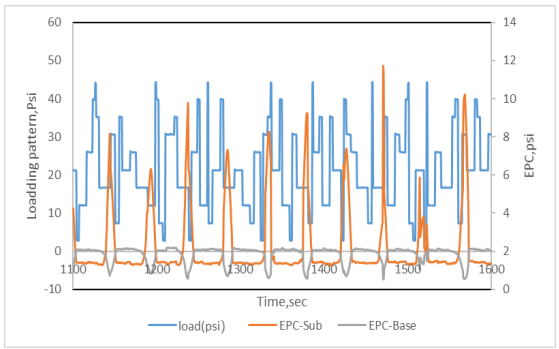

(d)

Figure 5-9 GE5- Loading vs. EPC: (a)Test details; (b) Overall EPC data vs. Time; (c) Loading pattern vs. EPC in time interval 0-500 second;(d) Loading pattern vs. EPC in time interval 1100-1600 second; (e) Loading pattern vs. EPC in time interval 27000-27500 second; (f) Loading pattern vs. EPC in time interval 40000-40500 second; (g) Loading pattern vs. EPC in time interval 60000-60500 second

www.manaraa.com

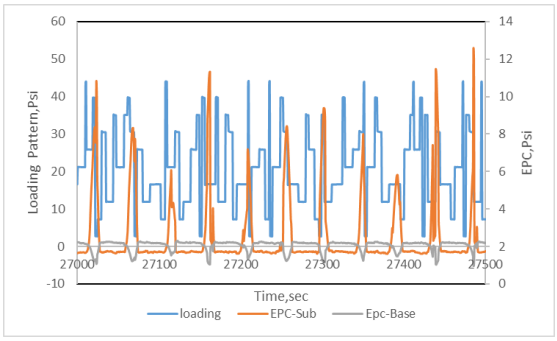

(e)

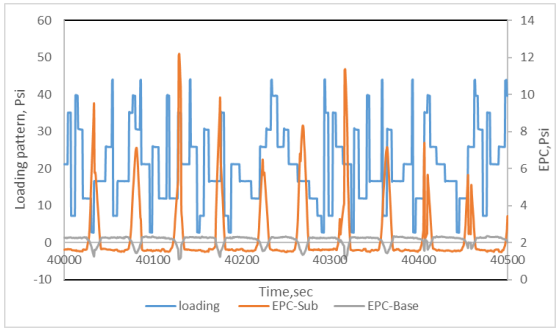

(f)

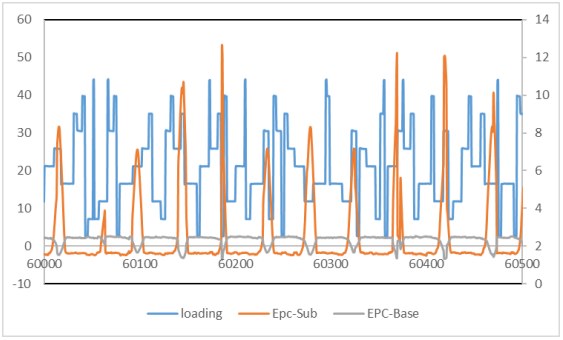

(g)

Figure 5-10. (continued)

GE 7

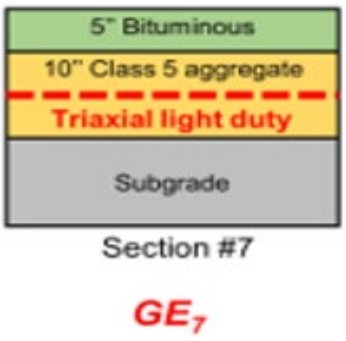

(a)

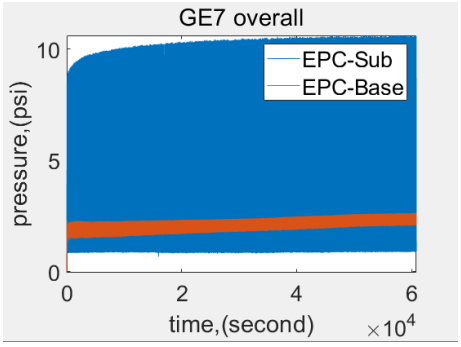

(b)

Figure 5-11 GE7- Loading vs. EPC: (a)Test details; (b) Overall EPC data vs. Time; (c) Loading pattern vs. EPC in time interval 0-500 second;(d) Loading pattern vs. EPC in time interval 2000-2500 second; (e) Loading pattern vs. EPC in time interval 30000-30500 second; (f) Loading pattern vs. EPC in time interval 45000-45500 second; (g) Loading pattern vs. EPC in time interval 60000-60500 second

www.manaraa.com

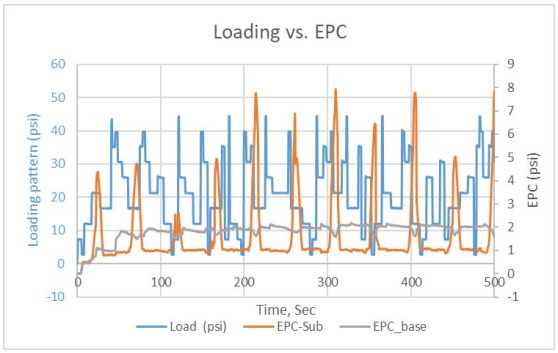

(c)

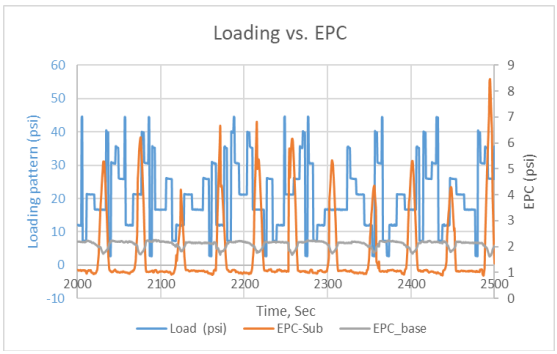

(d)

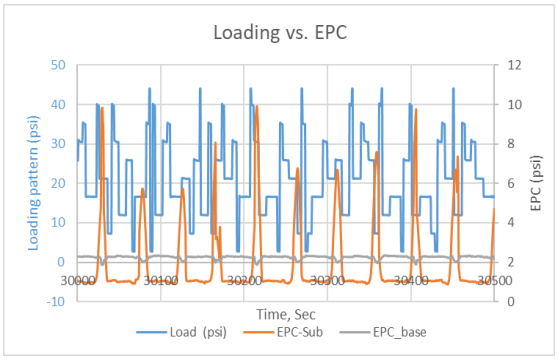

(e)

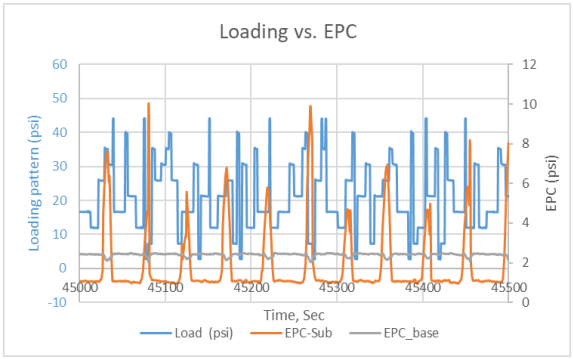

(f)

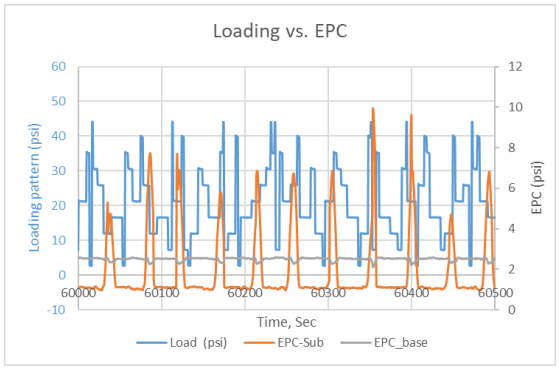

Figure 5-12. (continued)

www.manaraa.com

GE 12

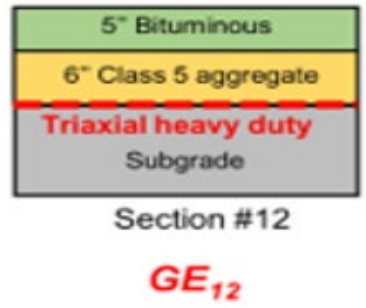

(a)

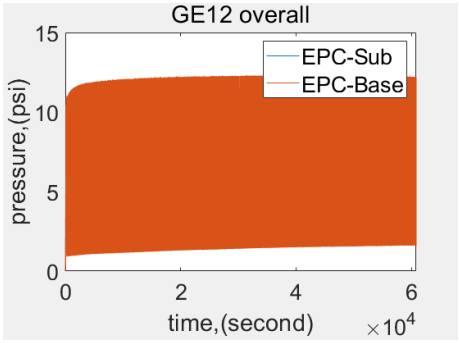

(b)

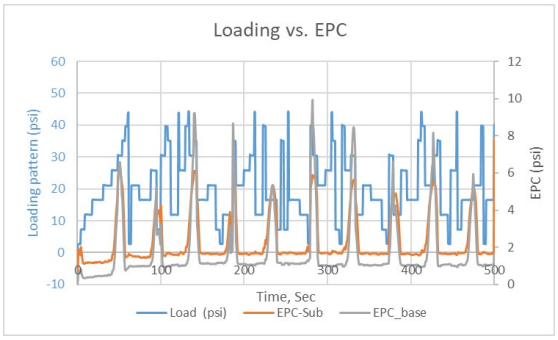

(c)

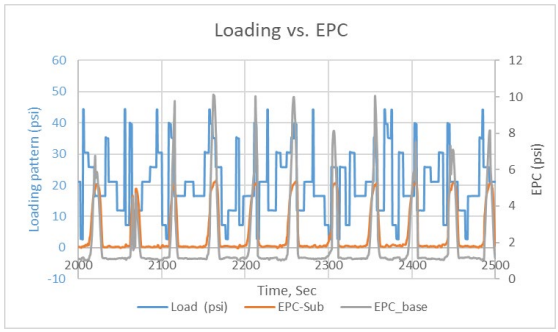

(d)

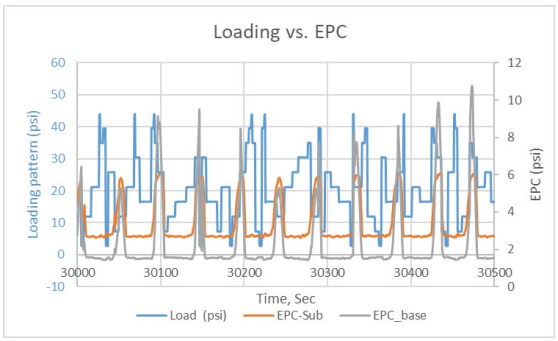

(e)

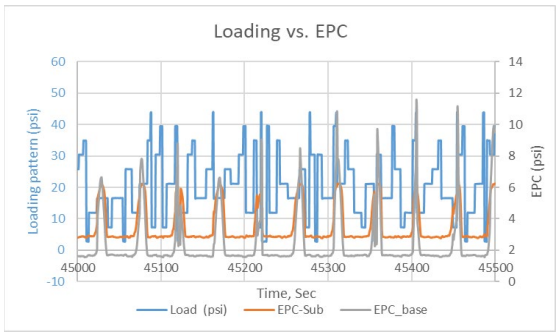

(f)

Figure 5-13 GE12- Loading vs. EPC: (a)Test details; (b) Overall EPC data vs. Time; (c) Loading pattern vs. EPC in time interval 0-500 second;(d) Loading pattern vs. EPC in time interval 2000-2500 second; (e) Loading pattern vs. EPC in time interval 30000-30500 second; (f) Loading pattern vs. EPC in time interval 45000-45500 second; (g) Loading pattern vs. EPC in time interval 60000-60500 second

www.manaraa.com

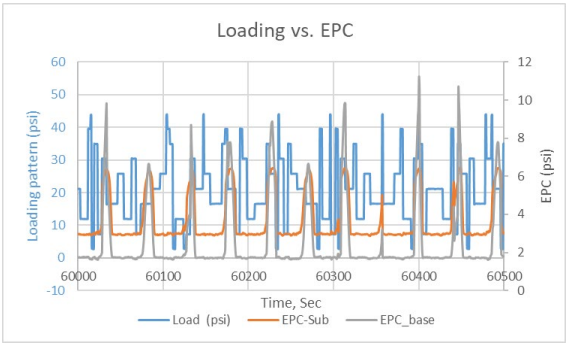

(g)

Figure 5-14. (continued)

GE 15

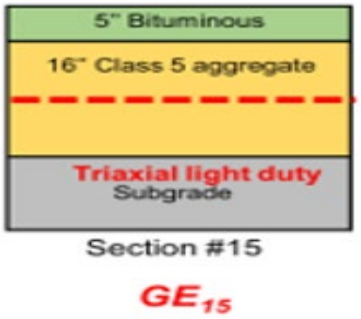

(a)

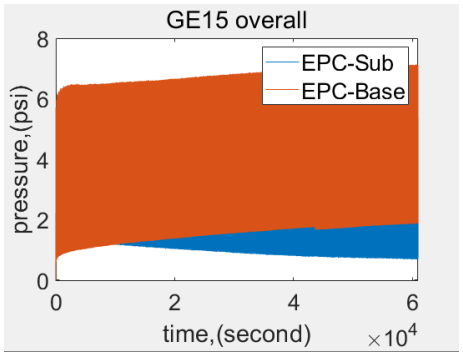

(b)

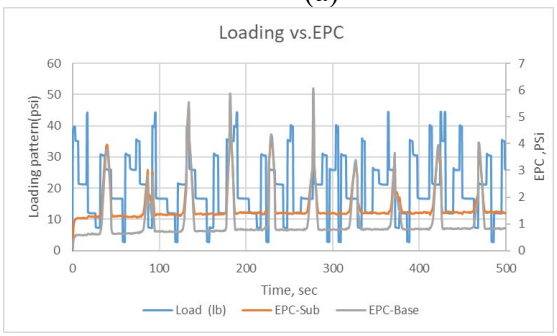

(c)

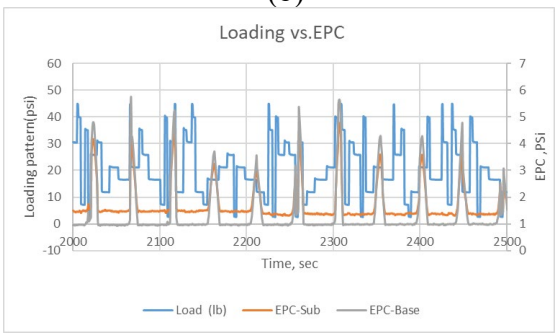

(d)

Figure 5-15 GE15- Loading vs. EPC: (a)Test details; (b) Overall EPC data vs. Time; (c) Loading pattern vs. EPC in time interval 0-500 second;(d) Loading pattern vs. EPC in time interval 2000-2500 second; (e) Loading pattern vs. EPC in time interval 30000-30500 second; (f) Loading pattern vs. EPC in time interval 45000-45500 second; (g) Loading pattern vs. EPC in time interval 60000-60500 second

www.manaraa.com

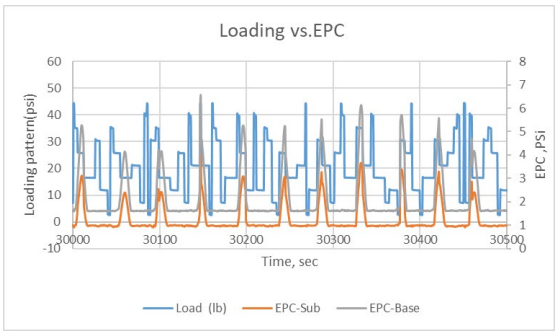

(e)

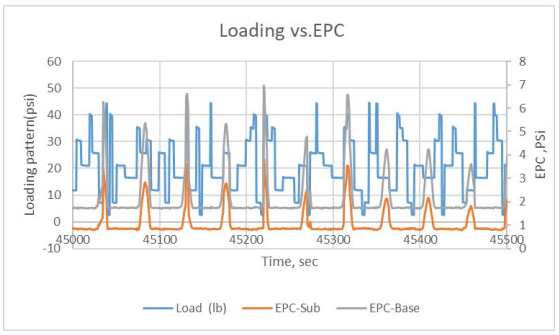

(f)

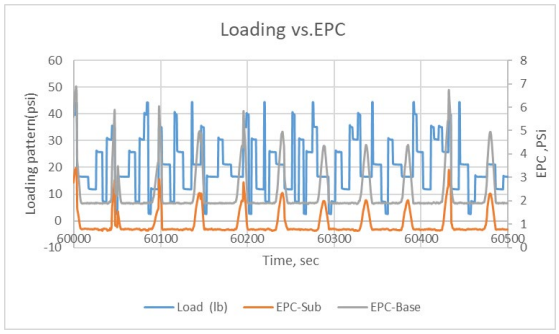

(g)

Figure 5-16. (continued)

Loading Pattern vs. Strain

GE 1

Direction 1 **Direction 2**

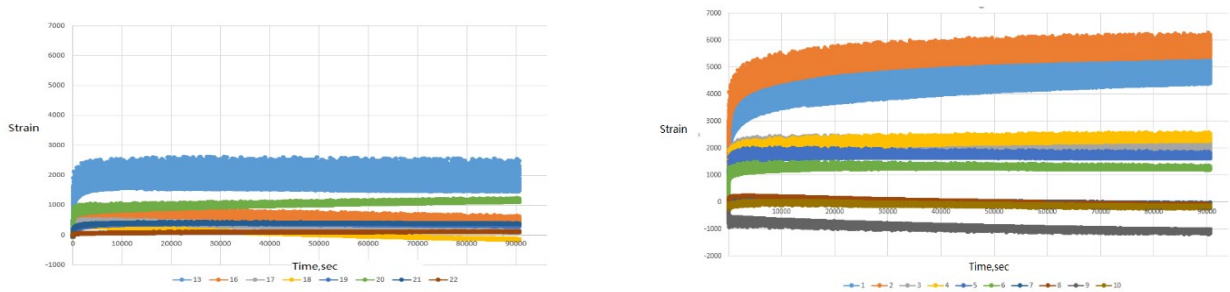

(a)

Figure 5-17 GE1 Loading Pattern vs. Strain for both direction: (a) Overall Strain vs. Time;(b) Time interval from 0-500 second; (c) Time interval from 2000-2500 second; (d) Time interval from 30000-30500 second; (e) Time interval from 45000-45500 second; (f) Time interval from 60000-60500 second

www.manaraa.com

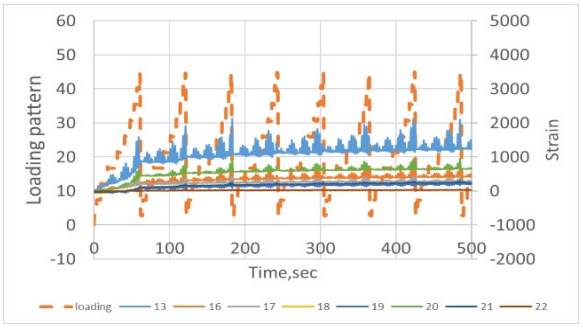

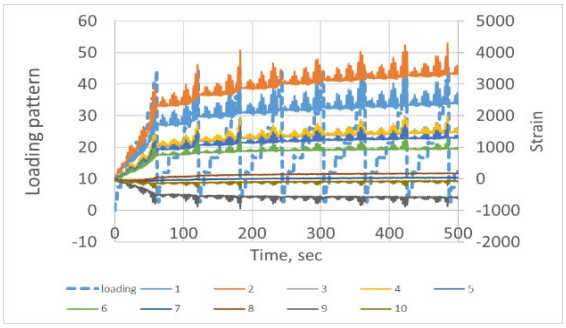

(b)

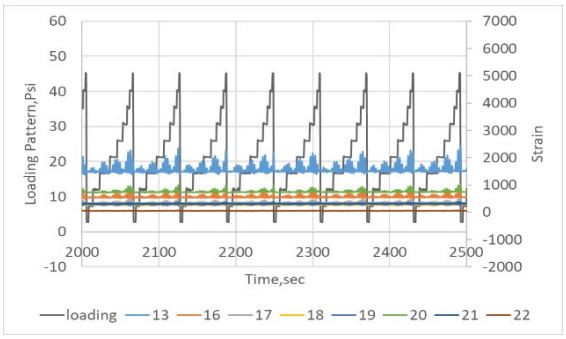

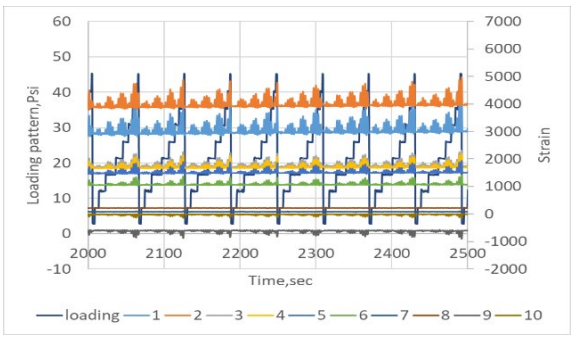

(c)

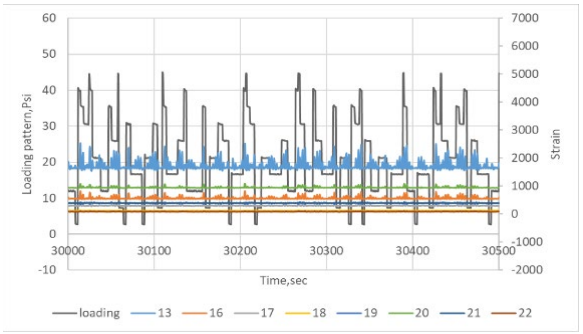

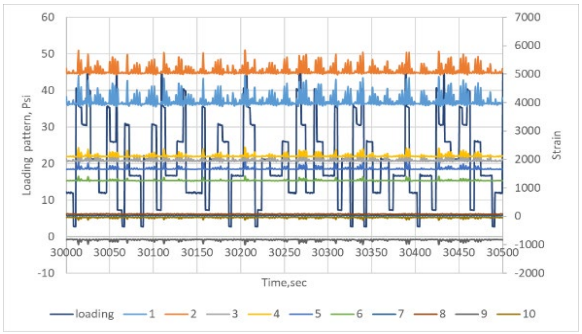

(d)

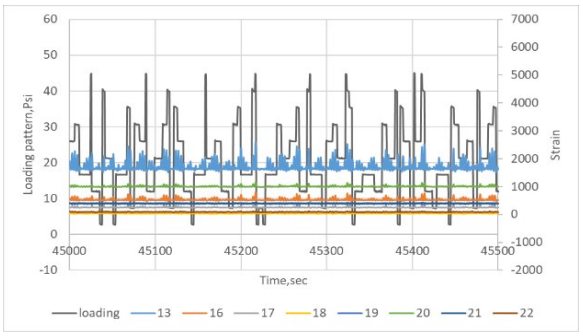

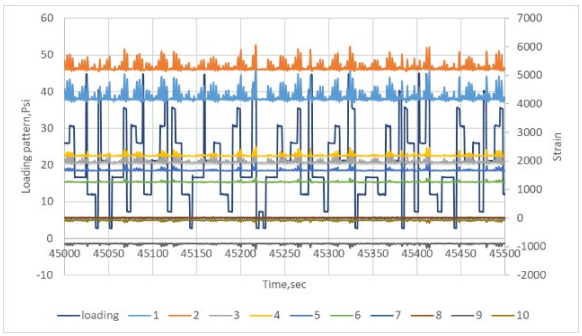

(e)

Figure 5-18. (continued)

www.manaraa.com

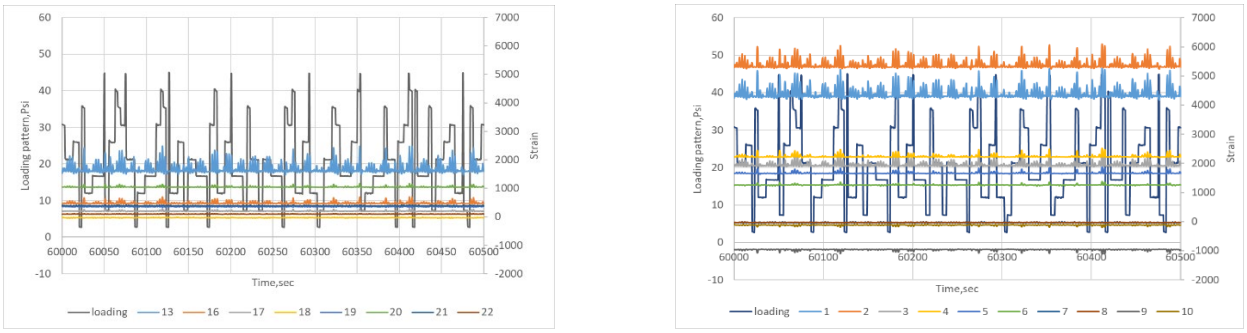

(f)

Figure 5-19. (continued)

GE 2

Direction 1 **Direction 2**

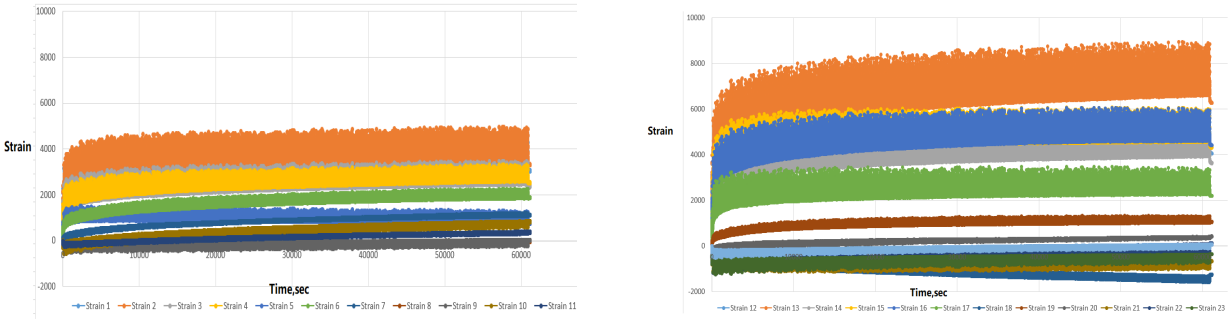

(a)

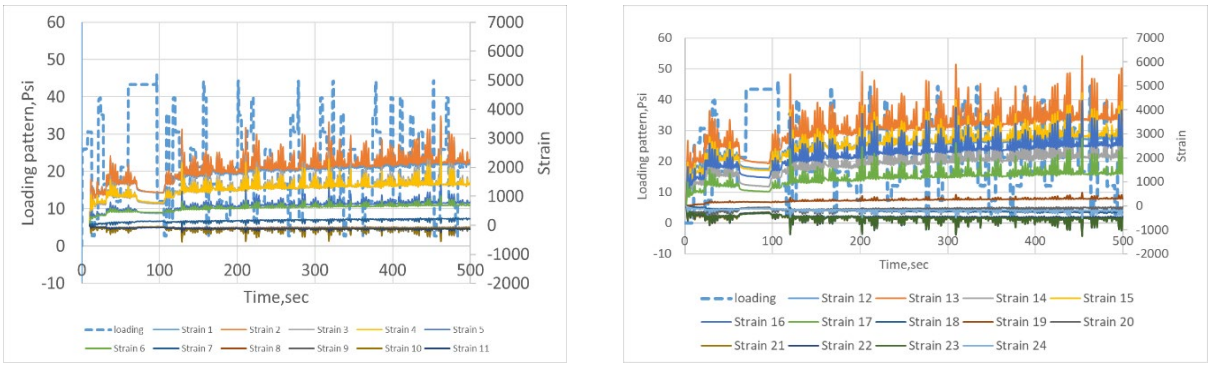

(b)

Figure 5-20 GE2 Loading Pattern vs. Strain for both direction: (a) Overall Strain vs. Time;(b) Time interval from 0-500 second; (c) Time interval from 2000-2500 second; (d) Time interval from 30000-30500 second; (e) Time interval from 45000-45500 second; (f) Time interval from 60000-60500 second

www.manaraa.com

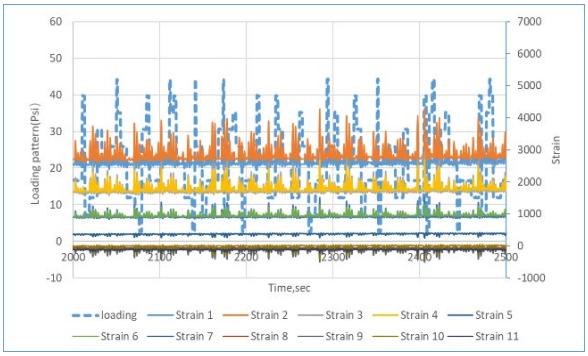

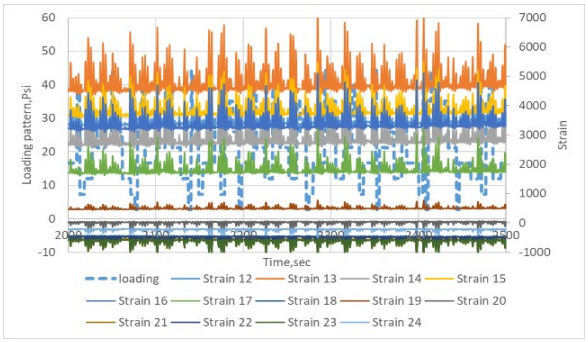

(c)

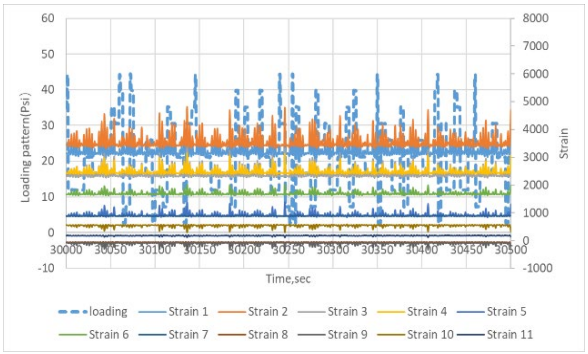

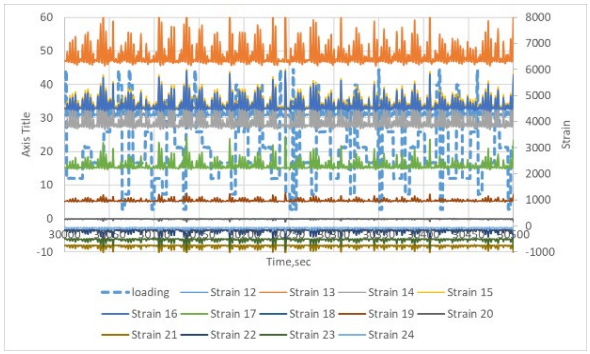

(d)

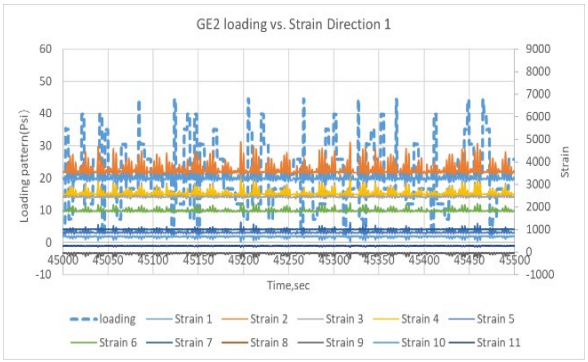

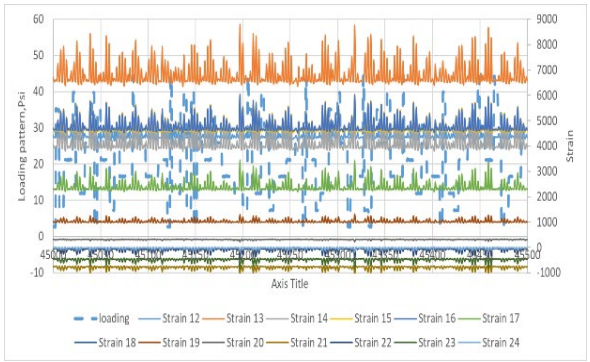

(e)

Figure 5-21. (continued)

www.manaraa.com

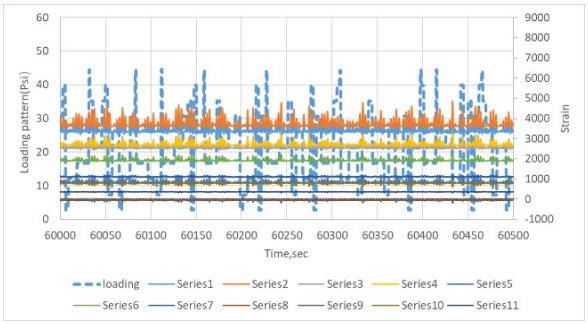

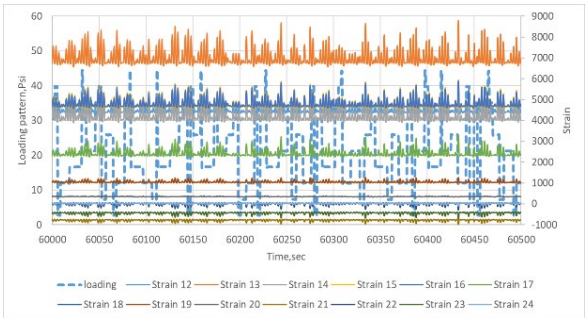

(f)

Figure 5-22. (continued)

GE 4

Direction 1 **Direction 2**

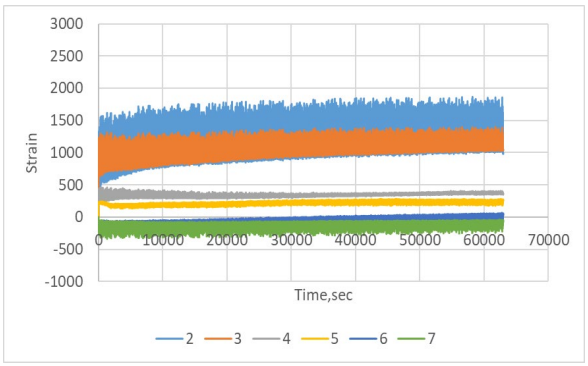

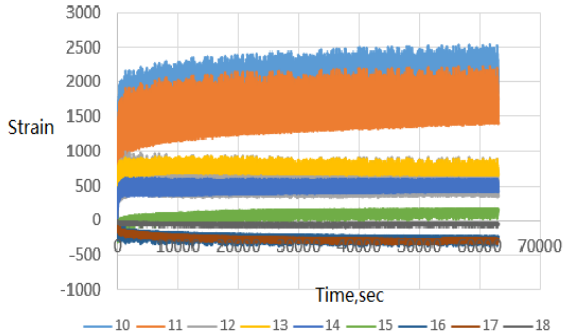

(a)

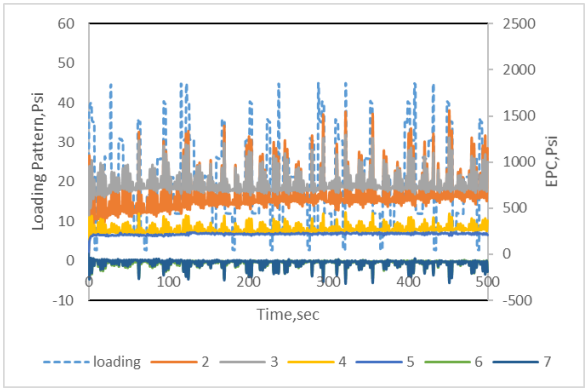

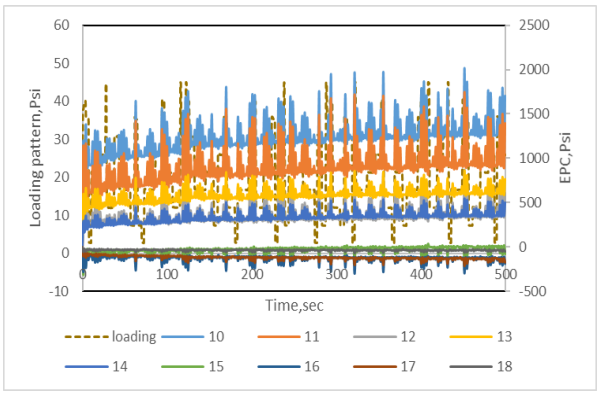

(b)

Figure 5-23 GE4 Loading Pattern vs. Strain for both direction: (a) Overall Strain vs. Time;(b) Time interval from 0-500 second; (c) Time interval from 2000-2500 second; (d) Time interval from 30000-30500 second; (e) Time interval from 45000-45500 second; (f) Time interval from 60000-60500 second

www.manaraa.com

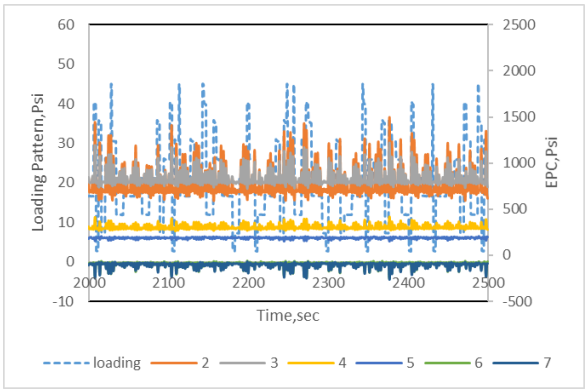

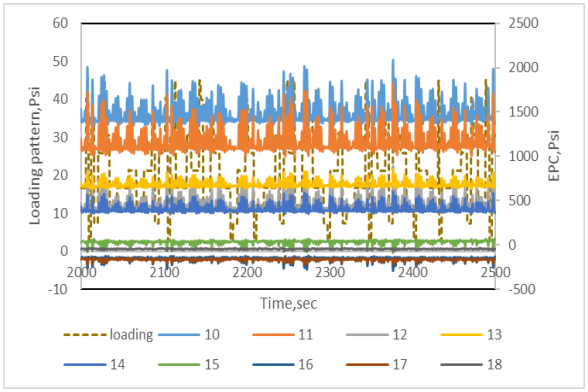

(c)

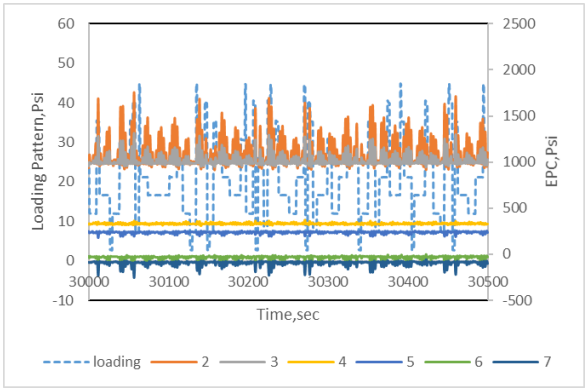

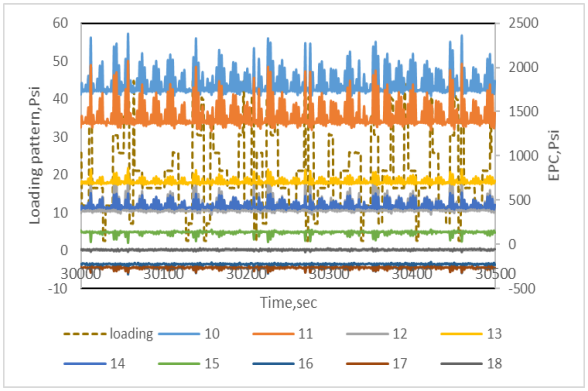

(d)

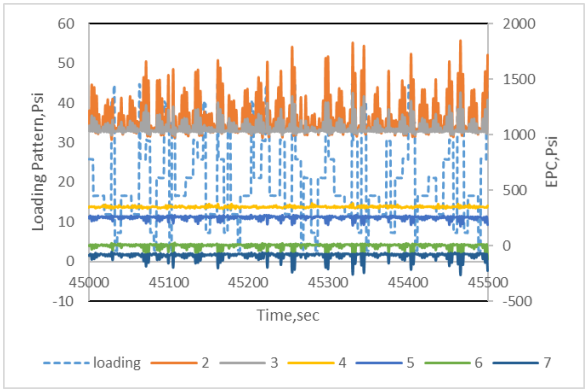

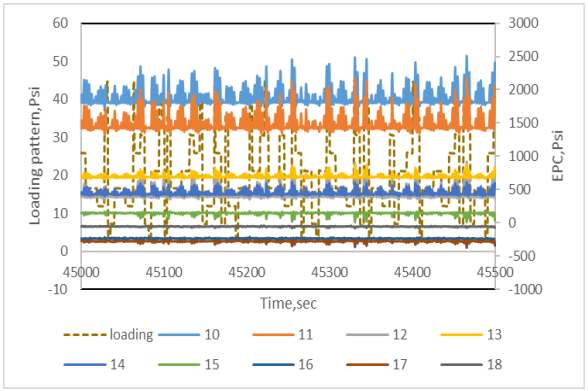

(e)

Figure 5-24. (continued)

www.manaraa.com

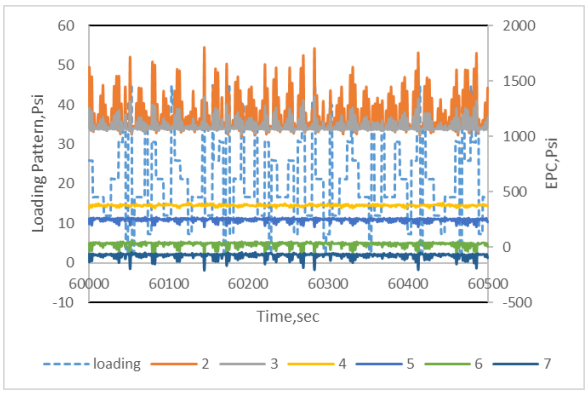

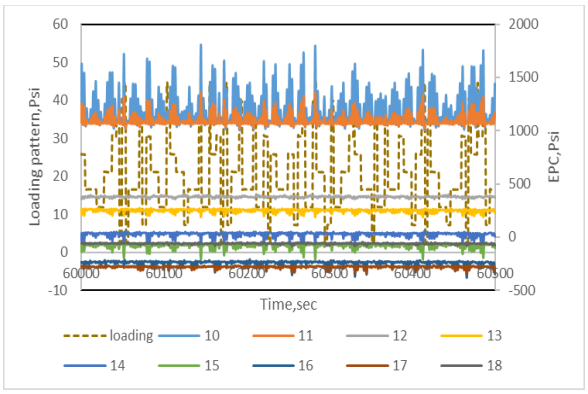

(f)

Figure 5-25. (continued)

GE 5

Direction 1 **Direction 2**

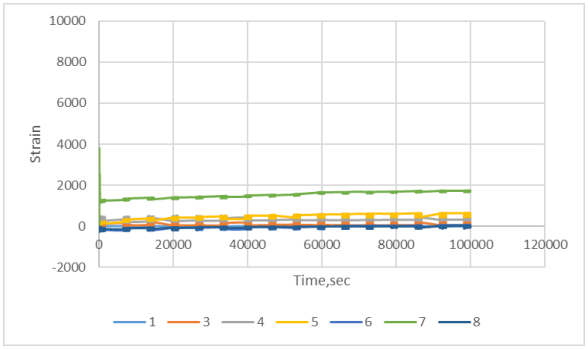

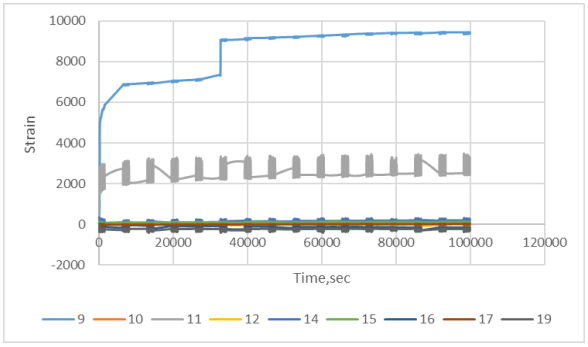

(a)

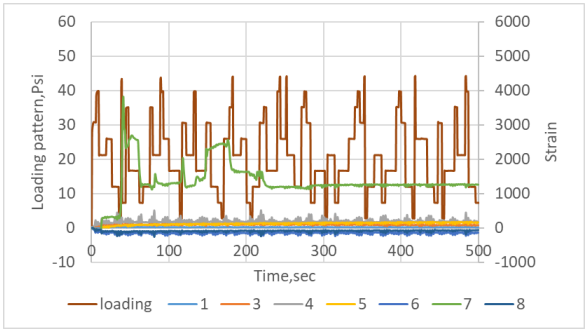

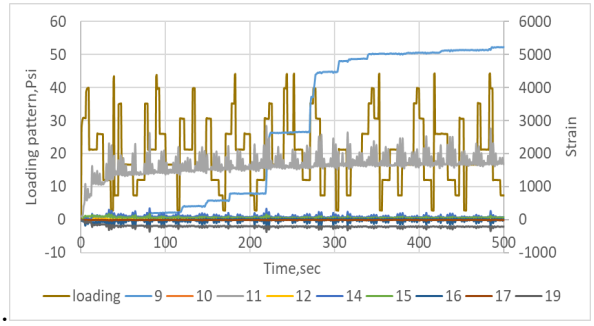

(b)

Figure 5-26 GE5 Loading Pattern vs. Strain for both direction: (a) Overall Strain vs. Time;(b) Time interval from 0-500 second; (c) Time interval from 2000-2500 second; (d) Time interval from 30000-30500 second; (e) Time interval from 45000-45500 second; (f) Time interval from 60000-60500 second

www.manaraa.com

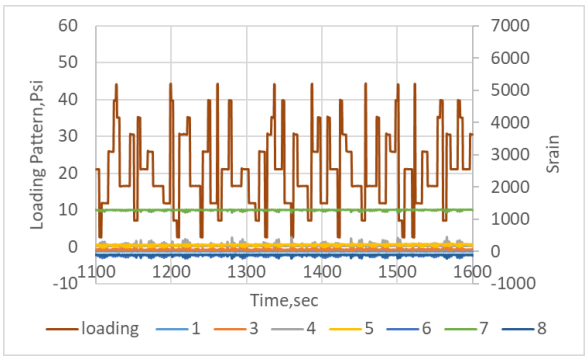

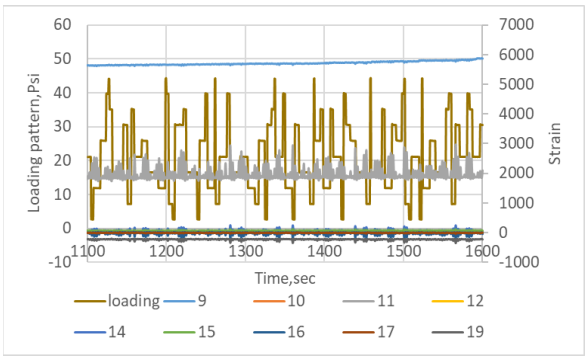

(c)

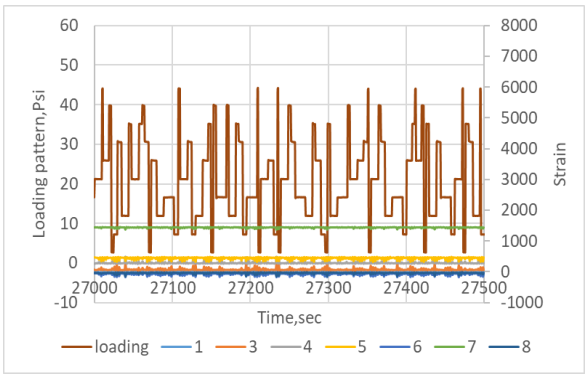

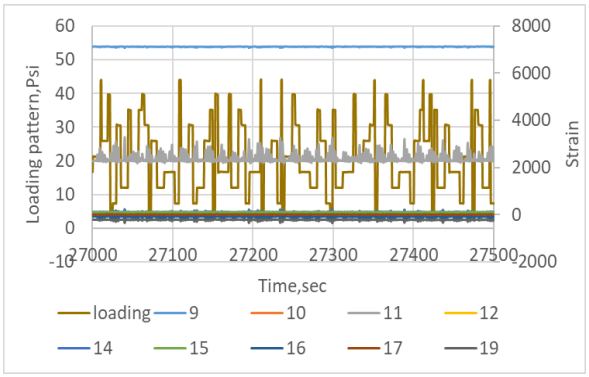

(d)

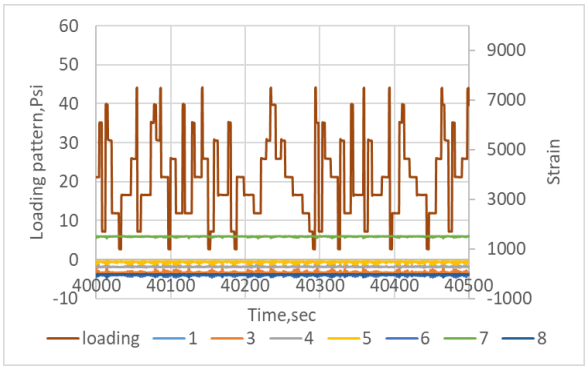

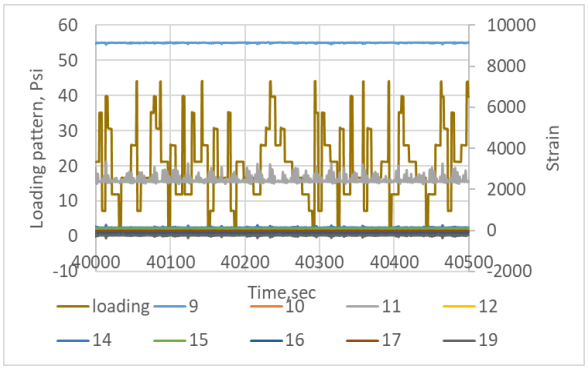

(e)

Figure 5-27. (continued)

www.manaraa.com

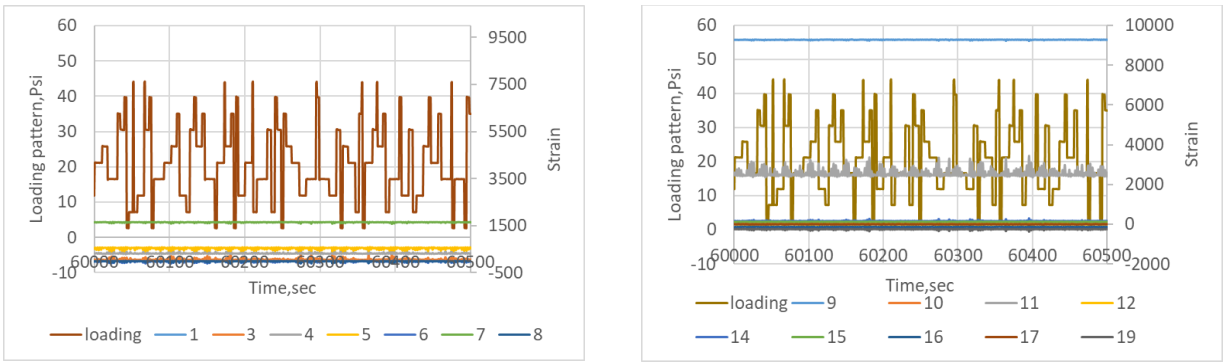

(f)

Figure 5-28. (continued)

GE 7

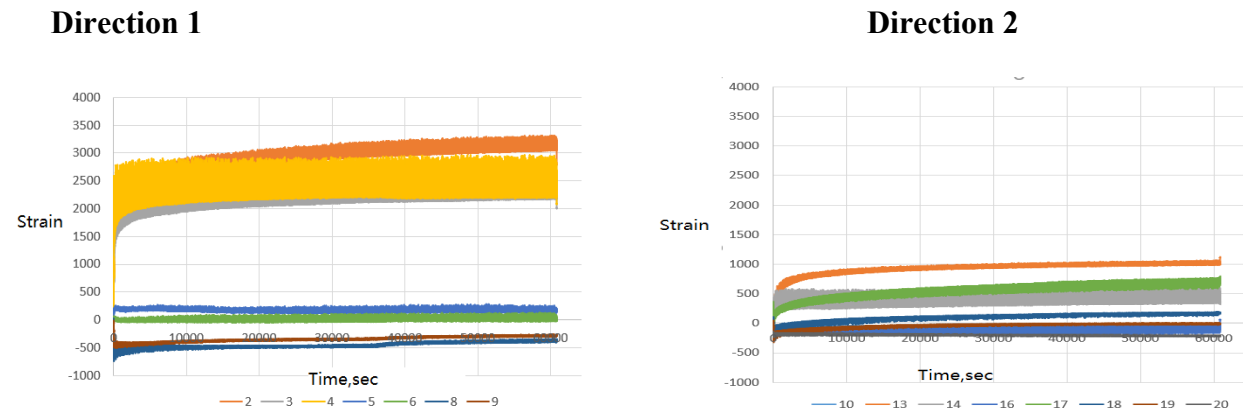

(a)

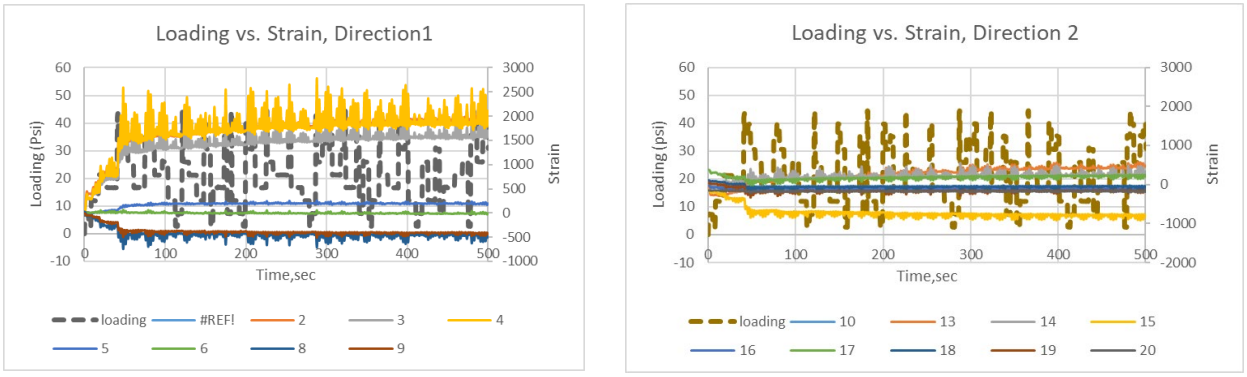

(b)

Figure 5-29 GE7 Loading Pattern vs. Strain for both direction: (a) Overall Strain vs. Time;(b) Time interval from 0-500 second; (c) Time interval from 2000-2500 second; (d) Time interval from 30000-30500 second; (e) Time interval from 45000-45500 second; (f) Time interval from 60000-60500 second

www.manaraa.com

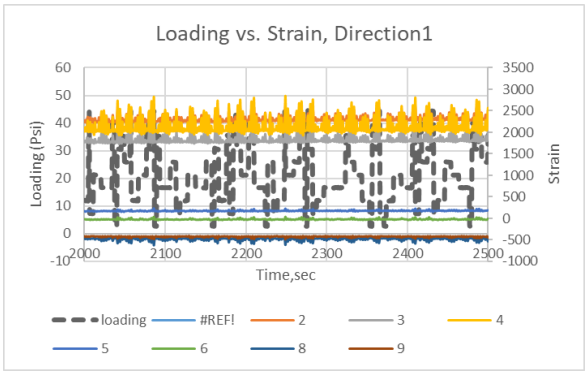

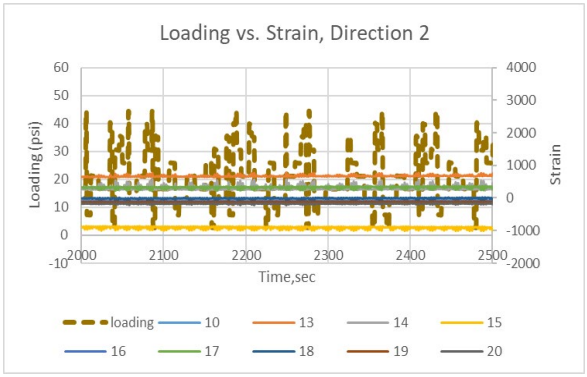

(c)

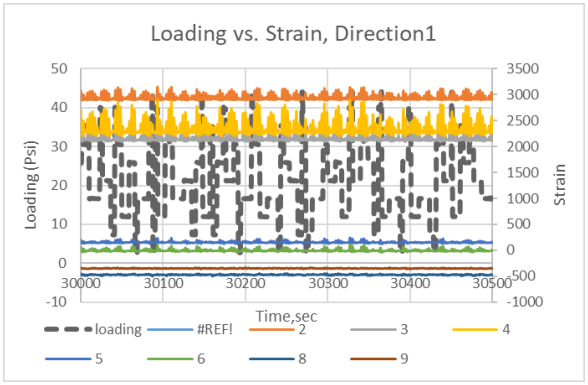

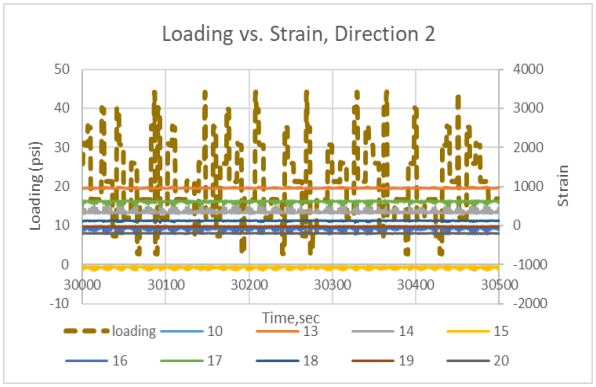

(d)

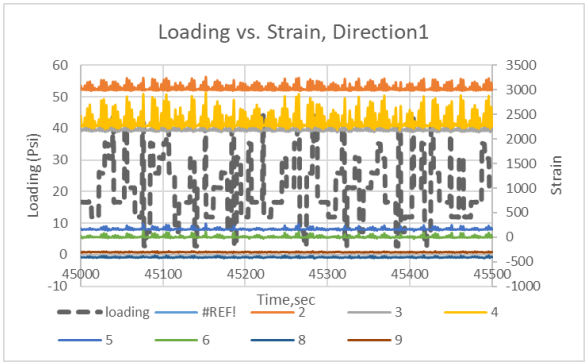

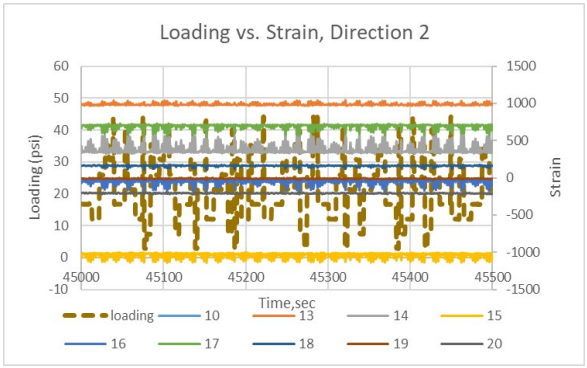

(e)

Figure 5-30. (continued)

www.manaraa.com

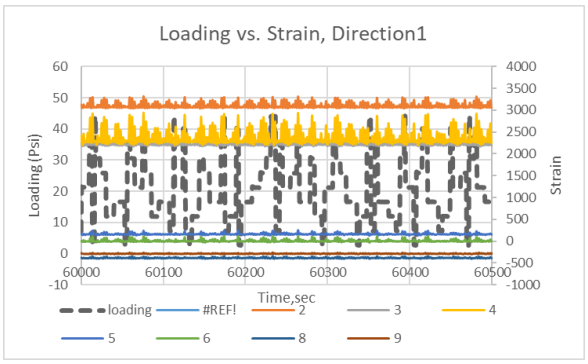

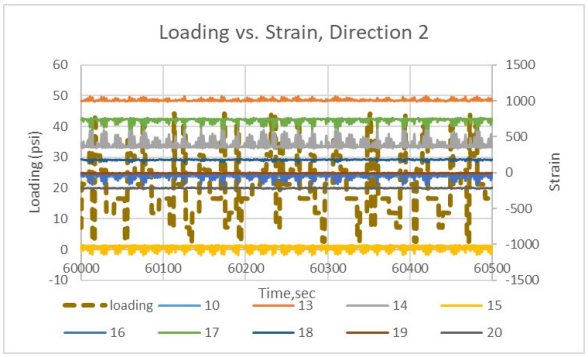

(f)

Figure 5-31.(continued)

GE 12

Direction 1 **Direction 2**

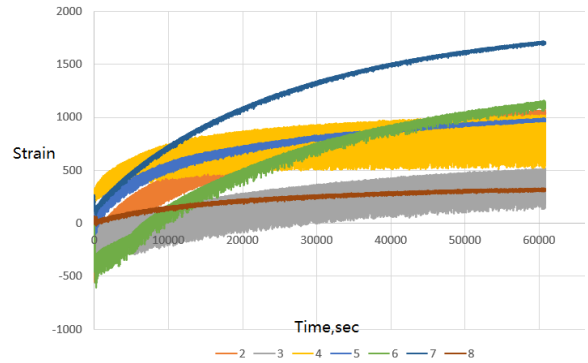

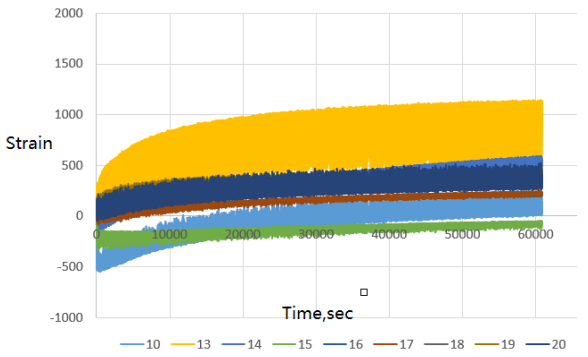

(a)

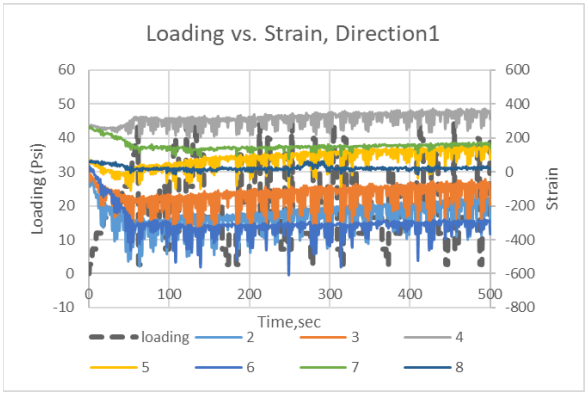

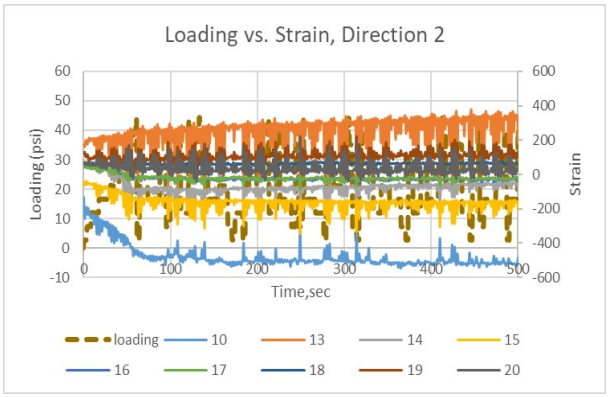

(b)

Figure 5-32 GE12 Loading Pattern vs. Strain for both direction: (a) Overall Strain vs. Time;(b) Time interval from 0-500 second; (c) Time interval from 2000-2500 second; (d) Time interval from 30000-30500 second; (e) Time interval from 45000-45500 second; (f) Time interval from 60000-60500 second

www.manaraa.com

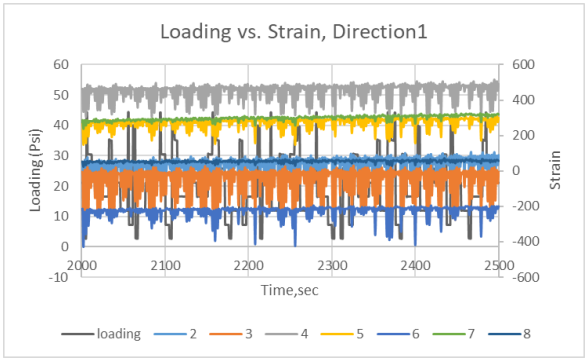

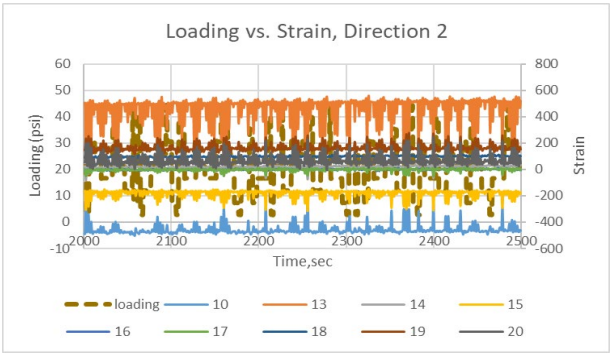

(c)

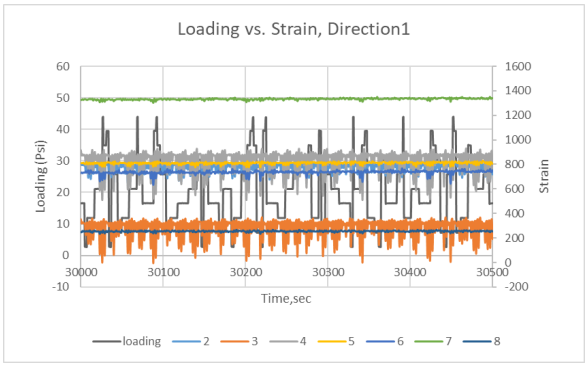

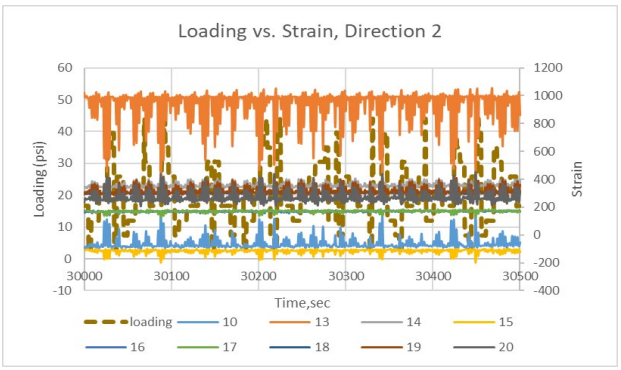

(d)

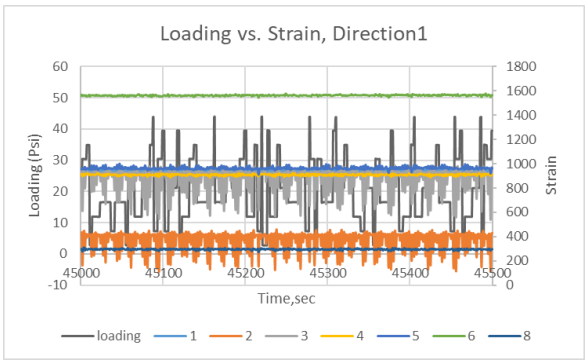

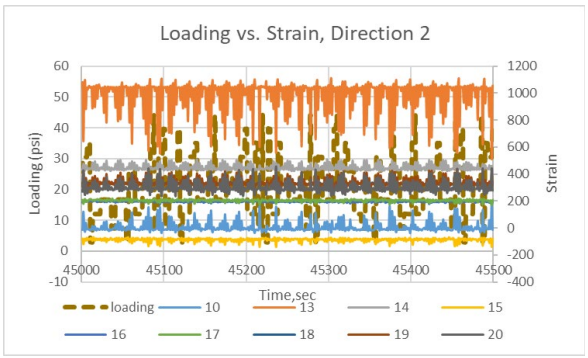

(e)

Figure 5-33. (continued)

www.manaraa.com

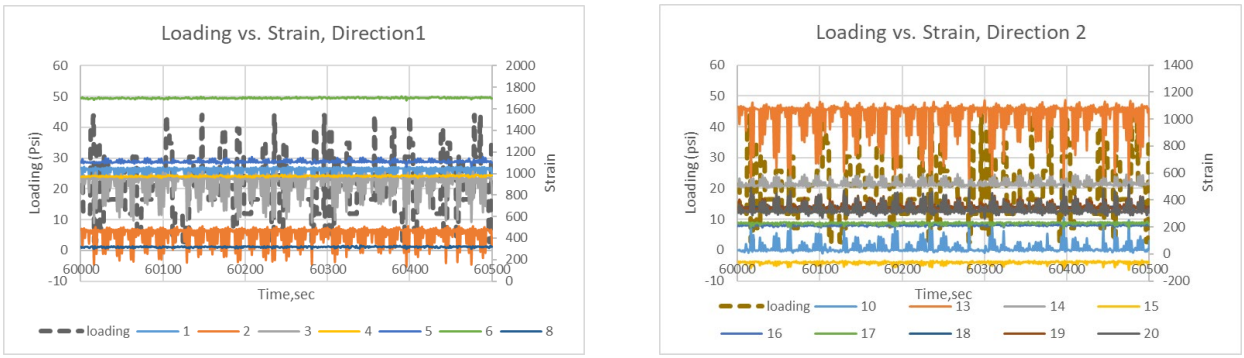

(f)

Figure 5-34. (continued)

GE 15

Direction 1 **Direction 2**

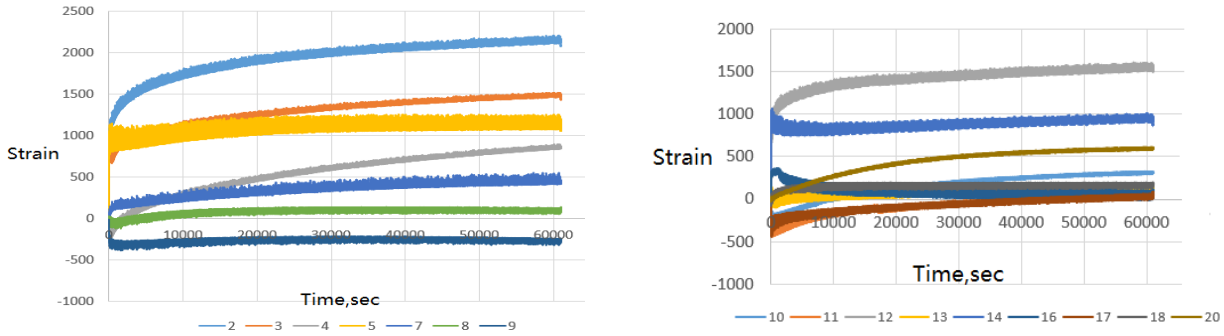

(a)

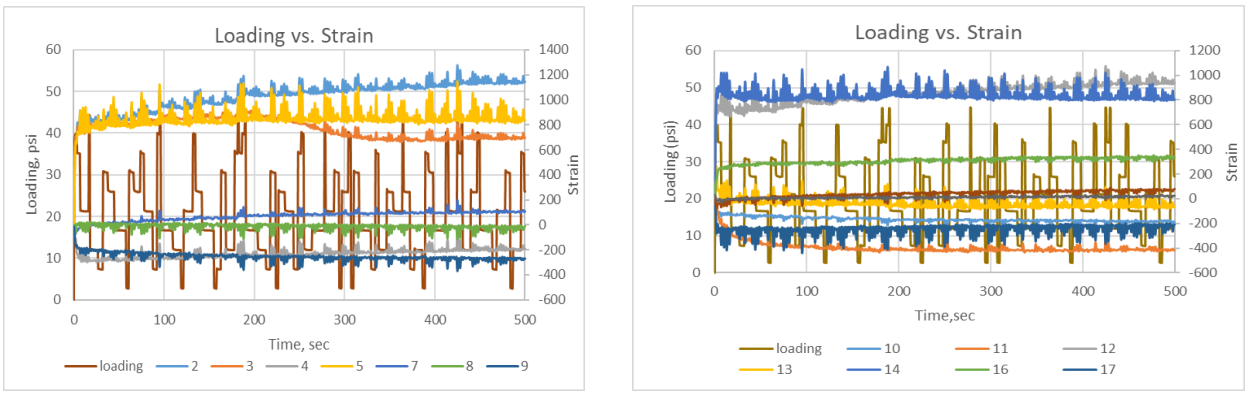

(b)

Figure 5-35 GE15 Loading Pattern vs. Strain for both direction: (a) Overall Strain vs. Time;(b) Time interval from 0-500 second; (c) Time interval from 2000-2500 second; (d) Time interval from 30000-30500 second; (e) Time interval from 45000-45500 second; (f) Time interval from 60000-60500 second

www.manaraa.com

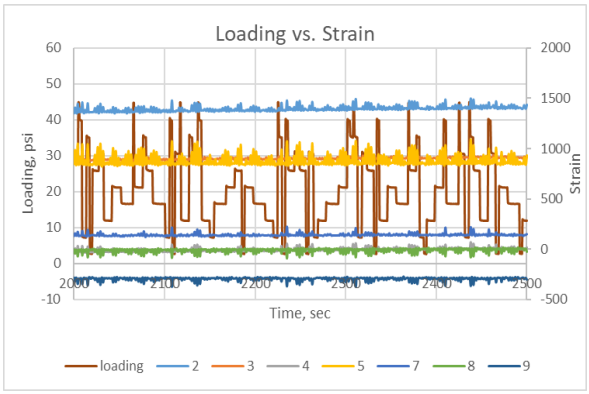

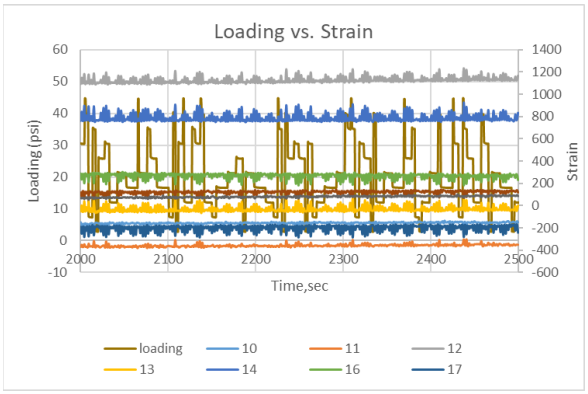

(c)

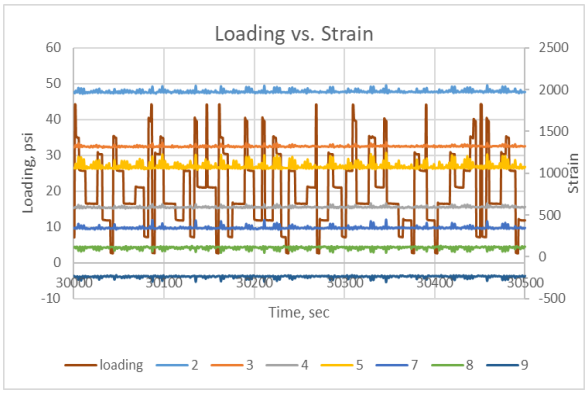

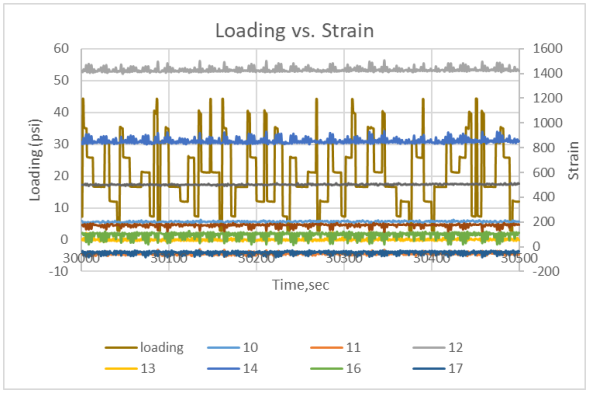

(d)

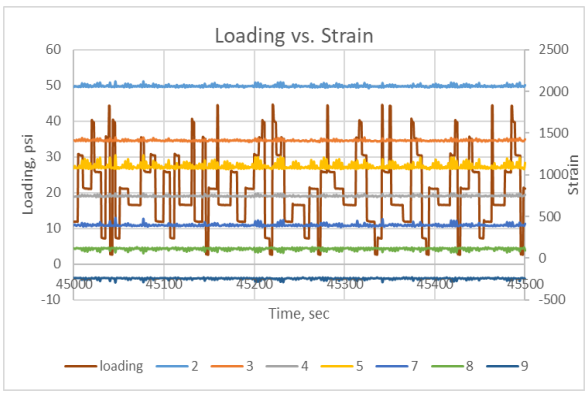

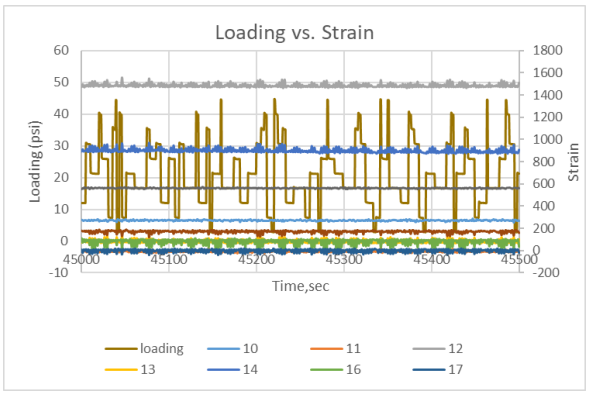

(e)

Figure 5-36. (continued)

www.manaraa.com

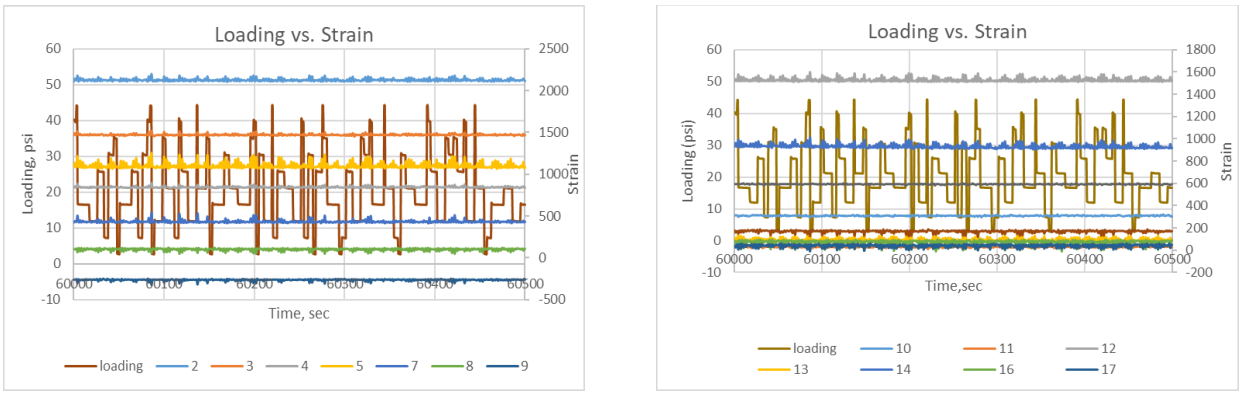

(f)

Figure 5-37. (continued)

Permanent Deformation

Figure 5-16 shows the permanent deformation verses the number of loading cycles. The deformation of the control section without the geogrid reaches almost 1 inch at the end of the test, which is the deepest deformation in the tests. In addition, the slope of the deformation curve is still going up which means the deformation might go larger.

GE2 and GE5 have the second largest deformation which are 0.58 in and 0.52, respectively. For these two sections, the trend of deformation curve is still increasing.

GE1, GE4, GE7, GE12 and GE15 have very similar result in deformation. The maximum deformation is around 0.25 inch for these sections. The deformation curves have very small slope which shows that the deformation is not going to increase rapidly.

www.manaraa.com

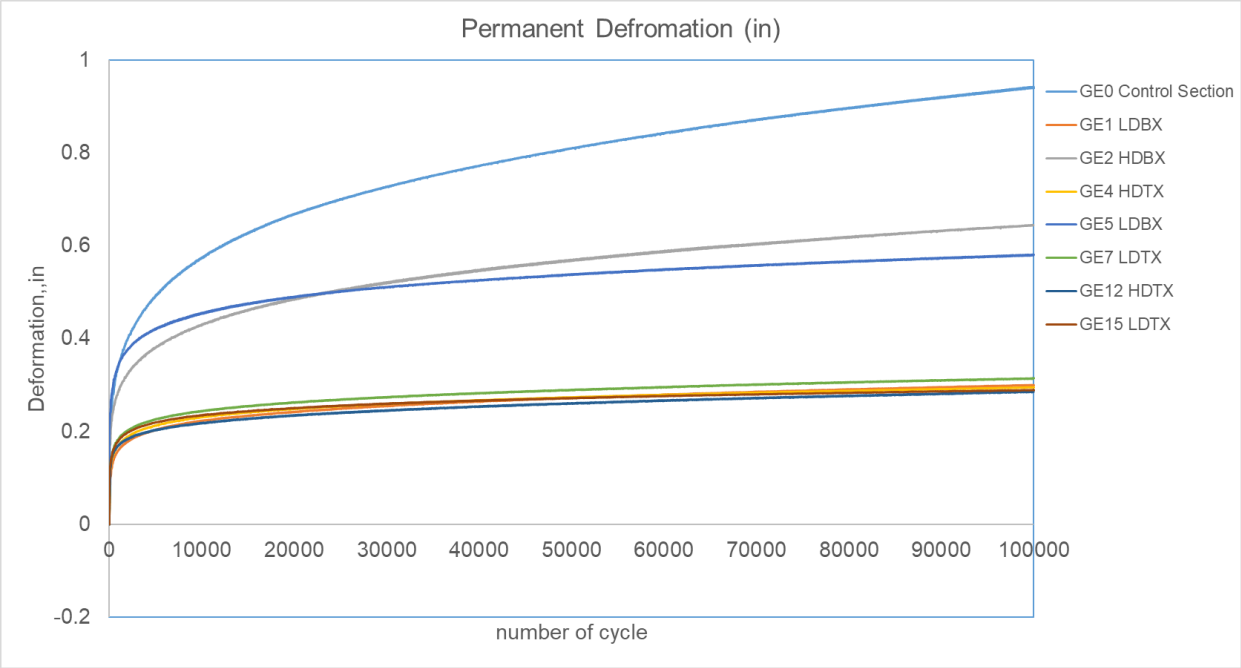

Figure 5-38 Permanent Deformation vs. Number of Cycles for Each Test Section

www.manaraa.com

CHAPTER 6. TEST RESULT ANALYSIS

- The test sections with the heavy-duty geogrid (list them in parentheses) always have the higher pressure cell data the light duty. For example, under the same location, the maximum pressure in GE1 with the light duty geogrid is 10psi; however, the maximum pressure in GE2 with the heavy duty can reach 15 psi. That's because the heavy duty geogrid has higher stiffness than the light duty geogrid, where more confinement can be provided by the high-strength geogrid.
- For all the overall EPC result except GE4 and GE7, the test sections have the similar trend: the earth pressure cell data was increasing as the loading enforces, both in the subgrade and base course layer, but the increasing rate and magnitude is higher in base course layer than the subgrade layer. This evidence supports the concept that the geogrid can stabilize both the subgrade and the base course layer, but more in base course. GE4 and GE7 have the converse result, and the reason could be caused by the geogrid location.
- For the geogrid placed at the interface between the subgrade and base course layer, the pressure cell data in base layer is always higher than the subgrade layer, which means the geogrid can provide more confinement force between the base course granular materials than the subgrade. By installing the geogrid in the middle of the base course layer, the geogrid cannot provide confining stress as at the interface. The location of the geogrid will have effect for the effectiveness of the geogrid.
- The average EPC data in Triaxial geogrid is higher than the Biaxial geogrid. The comparison between test section GE1 and GE4 on the EPC overall shows that under the

www.manaraa.com

same location and same thickness of base course layer, the pressure in 2psi higher than in GE4 than GE1. The Triaxial geogrid would have more effectiveness than the Biaxial.

- For the Triaxial geogrid, the strain results are similar in direction 1 and direction 2. Take GE4 as an example, the maximum strain in direction 1 is around 1.8% , and 2.3% in direction 2. The difference is less than 0.5% which could be neglected.
- However, for Biaxial geogrid, no matter where the geogrid was placed at the middle of the base course layer or the interface, the strain is always higher in direction 2 than direction 1. Take GE2 as an example, in direction 1, the maximum strain is 4%, and almost 9 % in direction 2. In direction 1, it's the transverse rib with shorter length, and it is the cross-machine direction with higher stiffness; In direction 2, it's the longitudinal rib with the longer length but lower stiffness, and it's the machine direction. The result from the strain data shows the longitudinal has the weaker strength and lower efficiency than the transverse rib in reinforcing the pavement. Figure 6-1 draws the relationship between the strength and the direction.

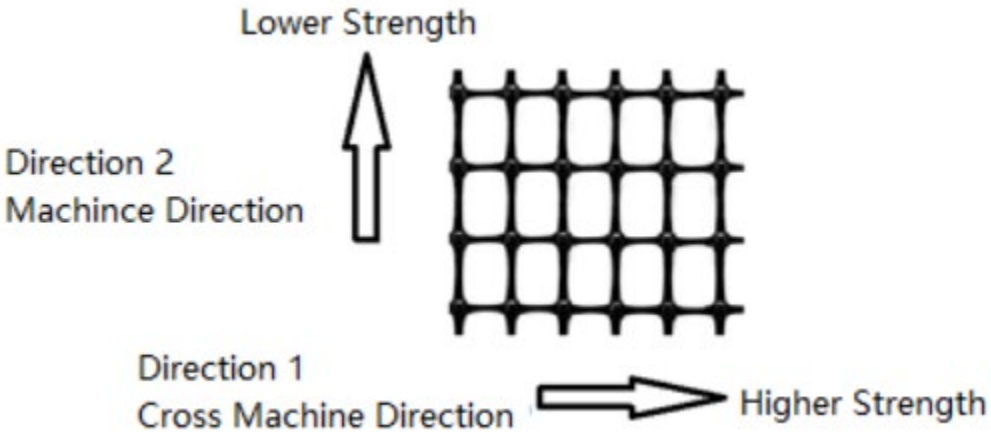

Figure 6-1 Relationship Between Direction and Strength in Biaxial Geogrid

www.manaraa.com

- By comparing the strain results and the pressure data from GE4 and GE12, it's found that GE4 has slightly higher strain data than GE12 in both direction; and the pressure in GE4 is slightly higher than GE 12 as well. The thickness of the base course layer is 10 inch in GE4 and 6 inch in GE12. This shows that the thickness of the base course layer has an effect on the behavior of the geogrid in reinforcement. More test sections need to be conducted to find out how the relationship between the base thickness and the effectiveness of the geogrid.

www.manaraa.com

CHAPTER 7. CONCLUSION

As one of the most popular geosynthetics products in geotechnical construction, geogrid is gaining popularity in roadway construction because of its excellent behavior in reinforcing the pavement. Geogrids can extend the service life of the pavement as well as decrease the cost of the project. In this study, a series of large-scale laboratory tests were conducted in order to determine the effectiveness of the geogrid under various parameters. These parameters include the types of geogrid, the aperture of the geogrid, the stiffness of the geogrid, the location where to install the geogrid, the thickness of the base course layer, etc.

With the use of the IMAS, eight laboratory tests were performed with different parameters. 100,000 cycles of random loading were simulated for each test sections, and the test data such as the permanent deformation, strain and the pressure were recorded by the instrumentations like pressure cell and strain gauges. Four type of geogrids were used with different stiffness and apertures. The thickness of the base course layer was 6 inches, 10 inches, and 16 inches for different test sections. After plotting and comparing these results, the main conclusions could be made below.

1. Heavy duty geogrids have more effectiveness than light duty in reinforcing the load. The test sections with heavy duty geogrid develop higher pressure than the light duty, thus more confinement was provided. The heavy-duty geogrid has better performance on stabilizing the base course layer than the light duty one based on the pressure data.
2. For Biaxial geogrids, direction 1, the cross-machine direction, has higher effectiveness than direction 2, the machine direction. The strain in direction 1 is only one half or one third as the strain in direction 2. The cross-machine direction in Biaxial geogrid can provide more strength for the pavement reinforcement.

www.manaraa.com

3. The Triaxial geogrids have more effectiveness than Biaxial. The strain results are two to three times higher in Biaxial than Triaxial geogrid. This result shows that the Biaxial geogrid has lower stiffness than the Triaxial. In addition, the pressure is also higher in Triaxial than Biaxial, which shows that Triaxial geogrid can provide more confining stress than Biaxial for Base course layer.

Although this is a successful study, some limitations still exist. Based on the findings of this study, the following recommendations are made if further studies need to be conducted: For testing the stain behavior for the Triaxial geogrid, strain gauges should be set for three directions instead of two, because the Triaxial geogrid is providing strength for all three direction. More test sections with different locations should be performed to find out how the location will affect the geogrid performance, such as 1/3 of the base layer. More test sections with different stiffness of base course should be tested as well, different base course material can be use such as the limestone.

www.manaraa.com

REFERENCES

Abu-Farsakh, M., & Nazzal, M. (2009, October). Evaluation of the Base/Subgrade Soil under Repeated Loading: Phase 1 – Laboratory Testing and Numerical Modeling of Geogrid Reinforced Bases in Flexible Pavement. Retrieved from https://www.ltrc.lsu.edu/pdf/2010/fr_450.pdf

Al-Arkawazi, S. A. (2017). Flexible Pavement Evaluation: A Case Study. Kurdistan Journal of Applied Research, 2(3), 292-301. doi:10.24017/science.2017.3.33

Brigham, D. (2019, July 17). The Best Geosynthetic for Pavement Separation/Stabilization. Retrieved July 19, 2020, from https://csengineermag.com/the-best-geosynthetic-for-pavement-separation-stabilization/

Castaneda, D. I., & Lange, D. A. (2012). New Field Testing Procedure to Measure Surface Stresses in Plain Concrete Pavements and Structures. *7th RILEM International Conference on Cracking in Pavements,* 191-200. doi:10.1007/978-94-007-4566-7_19

Chen, J., Yu, S., Xue, J., & Shi, Z. (2011). Experimental measurement and numerical computation of geogrid tension in centrifuge modeling. *KSCE Journal of Civil Engineering, 15*(8), 1343-1348. doi:10.1007/s12205-011-1071-6

Feng, X. J., Zuo, Z. Y., & Tong, W. (2014). Strain Measuring Techniques of the Geogrid. *Applied Mechanics and Materials, 578-579*, 1306-1310. doi:10.4028/www.scientific.net/amm.578-579.1306

Gnanendran, C., & Selvadurai, A. (2001). Strain measurement and interpretation of stabilising force in geogrid reinforcement. *Geotextiles and Geomembranes, 19*(3), 177-194. doi:10.1016/s0266-1144(01)00004-8

Hanandeh, S. (n.d.). Performance Evaluation of Instrumented Geosynthetics Reinforced Paved Test Sections Built Over Weak Subgrade Using Accelerated Load Testing. Retrieved July 19, 2020, from https://digitalcommons.lsu.edu/gradschool_dissertations/4421/

MnDOT.(2017). Grading and Base Manual. Retrieved June, 2020, from https://www.dot.state.mn.us/materials/manuals/GBase/2017gbmanual11032017.pdf

Saghebfar, M., Hossain, M., & Lacina, B. A. (2016). Performance of Geotextile-Reinforced Bases for Paved Roads. *Transportation Research Record: Journal of the Transportation Research Board, 2580*(1), 27-33. doi:10.3141/2580-04

Sharbaf, M. (2016, May). Laboratory Evaluation of Geogrid-Reinforced Flexible Pavements. Retrieved June, 2020, from https://digitalscholarship.unlv.edu/thesesdissertations/2737/

www.manaraa.com

Tensar. (2020). *Tensar Biaxial BX geogrids*. Retriveved from Tensar: https://www.tensarcorp.com/Systems-and-Products/Tensar-Biaxial-BX-geogrids

Tensar. (2020). *Tensar TriAx TX geogrids*. Retriveved from Tensar: https://www.tensarcorp.com/Systems-and-Products/Tensar-Triax-geogrid

Zornberg, J. G. (2017). Functions and Applications of Geosynthetics In Roadways. *Procedia Engineering, 189*, 298-306. doi:10.1016/j.proeng.2017.05.048

www.manaraa.com

APPENDIX A. PROPERTIES OF BASE SOILS

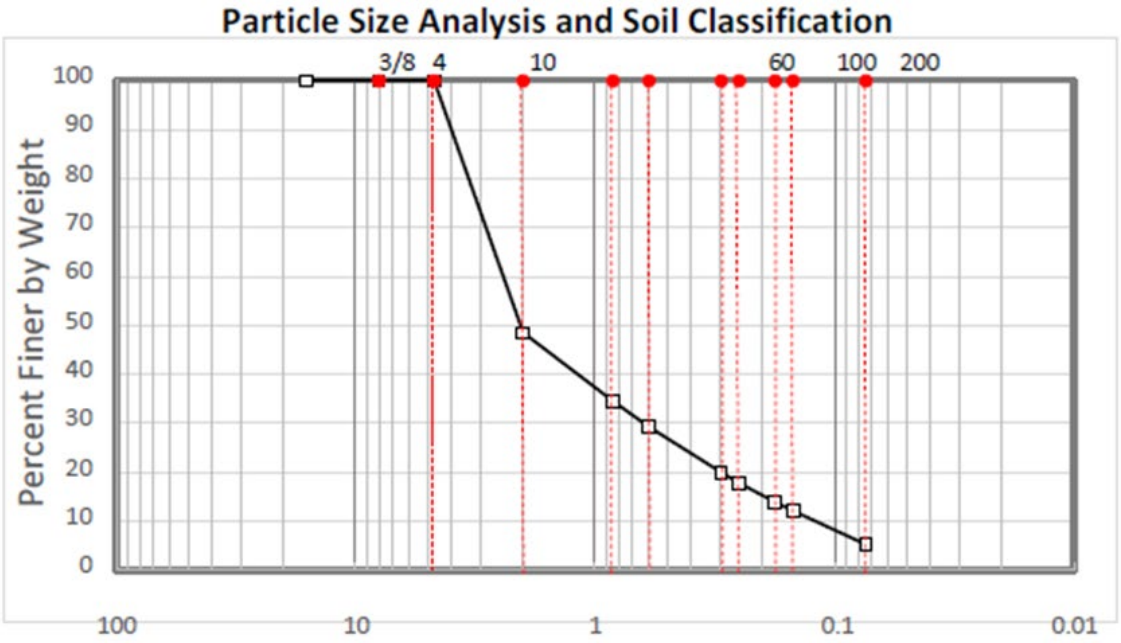

Materials

ID: Class 5 aggregates

Sample Location: Faribault, MN

Classification

AASHTO: A-1a

USCS: SM

Graduation Summary

% Gravel	0
% Sand	95
% Slit /Clay	5
D10(mm)	0.13
D30(mm)	0.6
D50(mm)	2.1
D60(mm)	2.5
Cu	19
Cc	1.1
D max	40.7

Atterberg Limit:

LL: 17.5

PL: N.P.

PI: -

Gradation and Soil Classification Test Results	
Project Name:	MnDOT NS555 Effectiveness of Geogrids
Project ID:	ISP-00007
Location:	142 Lab, Iowa State Univeristy

www.manaraa.com

APPENDIX B. PROPERTIES OF SUBGRADE SOILS

PARTICLE SIZE ANALYSIS AND SOIL CLASSIFICTAION

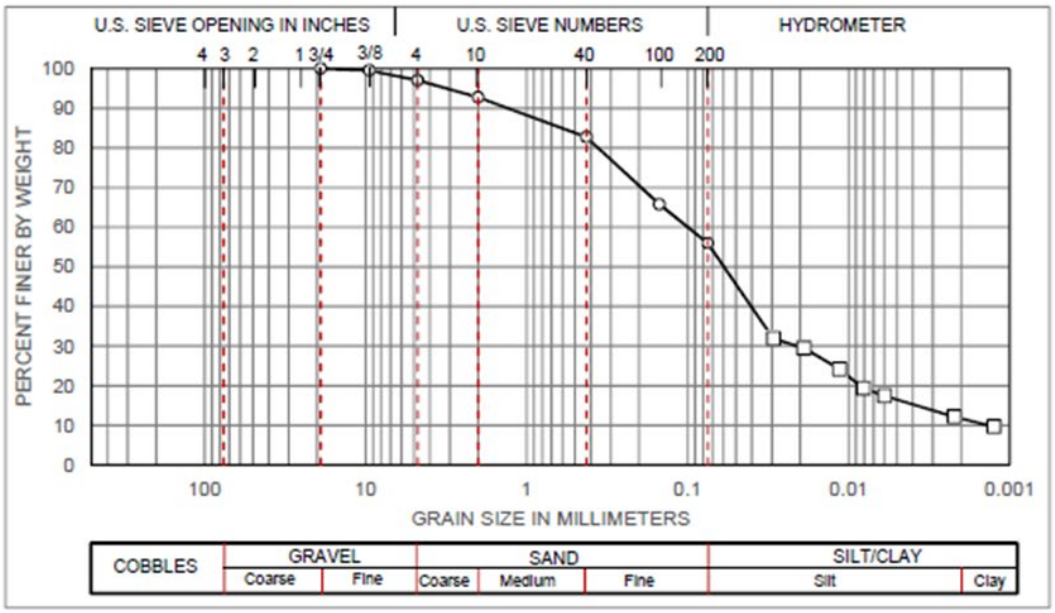

Material

ID:	Fairbault Clay
Sample Location:	Fairbault, MN

Classification

AASHTO[1]:	A-7-6 (2)
USCS[2]:	CL (Sandy Lean Clay)

Gradation Summary[3]

% Gravel	3.0
% Sand	41.1
% Silt	44.4
% Clay	11.6
D_{10} (mm)	0.001
D_{30} (mm)	0.021
D_{50} (mm)	0.064
D_{60} (mm)	0.106
D_{85} (mm)	0.782
C_u	76.35
C_c	3.08

Atterberg Limits[4]

LL	30
PL	22
PI	8

[1]ASTM D3282-15
[2]ASTM D2487-17
[3]ASTM D422-63
[4]ASTM D4318-17

Gradation and Soil Classification Test Results

Project Name:	MnDOT NS555 Effectiveness of Geogrids
Project ID:	ISP-00007
Location:	Ingios Lab, Northfield, MN

ingios GEOTECHNICS

www.manaraa.com